Journal of Medicinal Chemistry

pubs.acs.org/jmc Article

Discovery of M-1121 as an Orally Active Covalent Inhibitor of Menin-MLL Interaction Capable of Achieving Complete and Long-Lasting Tumor Regression

Meng Zhang,[±] Angelo Aguilar,[±] Shilin Xu,[±] Liyue Huang,[±] Krishnapriya Chinnaswamy, Taryn Sleger, Bo Wang, Stefan Gross, Brandon N. Nicolay, Sebastien Ronseaux, Kaitlin Harvey, Yu Wang, Donna McEachern, Paul D. Kirchhoff, Zhaomin Liu, Jeanne Stuckey, Adriana E. Tron, Tao Liu, and Shaomeng Wang*

Cite This: *J. Med. Chem.* 2021, 64, 10333−10349 Read Online

ACCESS | Metrics & More | Article Recommendations | Supporting Information

ABSTRACT: Targeting the menin-MLL protein−protein interaction is being pursued as a new therapeutic strategy for the treatment of acute leukemia carrying MLL-rearrangements (MLLr leukemia). Herein, we report M-1121, a covalent and orally active inhibitor of the menin-MLL interaction capable of achieving complete and persistent tumor regression. M-1121 establishes covalent interactions with Cysteine 329 located in the MLL binding pocket of menin and potently inhibits growth of acute leukemia cell lines carrying MLL translocations with no activity in cell lines with wild-type MLL. Consistent with the mechanism of action, M-1121 drives dose-dependent down-regulation of *HOXA9* and *MEIS1* gene expression in the MLL-rearranged MV4;11 leukemia cell line. M-1121 is orally bioavailable and shows potent antitumor activity *in vivo* with tumor regressions observed at tolerated doses in the MV4;11 subcutaneous and disseminated models of MLL-rearranged leukemia. Together, our findings support development of an orally active covalent menin inhibitor as a new therapy for MLLr leukemia.

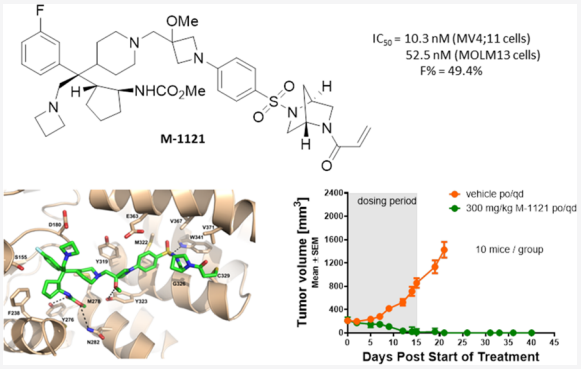

INTRODUCTION

Chromosomal translocations of the mixed lineage leukemia 1 (MLL1, also known as MLL) are found in 5−10% of acute leukemias in adults and in approximately 70% of acute lymphoid leukemia (ALL) in infants.[1,2] Acute myeloid leukemias (AML) carrying MLL rearrangements (MLLr leukemia) have poor clinical prognosis with a 5 year survival rate of about 35%.[1,2] MLLr leukemias are resistant to current therapies, highlighting the need for developing new therapeutic strategies for this disease.

Upon chromosomal translocations, the MLL gene is fused with one of over 80 partner genes, resulting in chimeric genes that encode oncogenic MLL fusion proteins.[4] The protein−protein interaction between these MLL fusion proteins and the oncogenic co-factor menin is critical for overexpression of *MEIS1* and *HOXA* genes that led to the development and maintenance of MLLr leukemia.[5−9] Thus, targeting the menin-MLL protein−protein interaction is being pursued as a new therapeutic strategy for MLLr leukemia.[3,8,10−13] To date, potent small-molecule inhibitors of the menin-MLL protein−protein interaction (hereafter called menin inhibitors, Figure 1) have been reported.[14−28] Two of those small-molecule inhibitors have been advanced into early-phase clinical development, and encouraging early clinical activities have been recently reported for both compounds.[31,32]

In 2018, we published the structure-based discovery of M-525, the first-in-class, potent, covalent small-molecule menin inhibitor.[26] We demonstrated that M-525 is more potent than its noncovalent inhibitor counterparts in reducing the expression of *HOXA9* and *MEIS1* genes and in inhibiting growth of leukemia cells carrying MLL translocations. Optimization of M-525 yielded M-808,[28] a potent, covalent menin inhibitor with antitumor activity in *in vitro* and in *in vivo* models of MLLr leukemia (Figure 1). Despite its superior cellular potency, M-808 was discontinued for further development due to the low oral bioavailability demonstrated in mice. In this study, we describe our efforts to further improve M-808 oral bioavailability, which resulted in the discovery of M-1121 as the first, potent, and orally active covalent menin inhibitor,

Received: April 30, 2021
Published: July 1, 2021

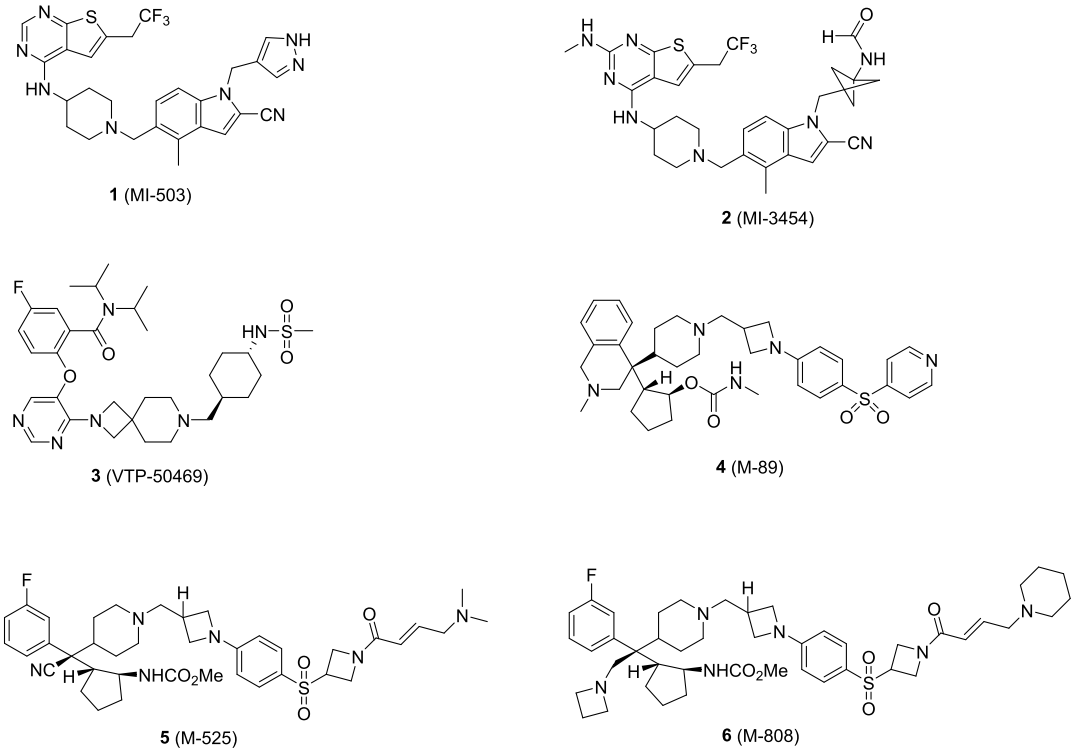

Figure 1. Representative menin inhibitors.

capable of achieving complete and long-lasting tumor regression.

RESULTS AND DISCUSSION

Design and Synthesis of New Noncovalent Menin Inhibitors. As can be seen from the chemical structures of M-525 and M-808 in Figure 1, a covalent menin inhibitor consists of a noncovalent menin-binding scaffold and an electrophile for the formation of a covalent bond with a cysteine residue in menin. We reasoned that superior oral bioavailability for a covalent inhibitor could be achieved by improving the oral bioavailability of the noncovalent portion of the molecule. We modified the inhibitor portion of M-525 and M-808 lacking the electrophile group to first obtain a potent and orally bioavailable noncovalent inhibitor that could later be added an electrophile group for establishing covalent interactions.

Based upon M-525, compound **7** lacking an electrophile was designed and synthesized as a noncovalent menin inhibitor. Compound **7** binds to menin with an IC_{50} value of 6.9 nM as determined by the fluorescence polarization (FP)-based competitive binding assay.[27] This compound was then tested for its ability to inhibit cell proliferation of the acute leukemia cell lines MV4;11 and MOLM-13 carrying MLL-AF4 and MLL-AF9 fusion, respectively. Compound **7** showed moderate antiproliferative activities in MV4;11 and MOLM-13 cells with IC_{50} values of 798 and 840 nM, respectively.

Based on the co-crystal structure of the M-808-menin complex, the positively charged amino group in M-808 establishes charge−charge interaction with the negatively charged carboxyl group of Asp180.[12] Accordingly, we have synthesized and evaluated a series of new menin inhibitors containing different positively charged groups, with the results summarized in Table 1.

Compound **8** containing a primary amino group binds to menin with an IC_{50} value of 4.0 nM and inhibits cell growth

Table 1. Binding Affinity and Cell Growth Inhibition Values of Menin Inhibitors (7−13)

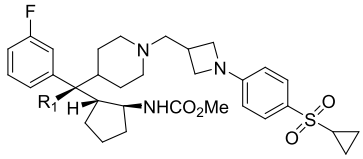

Compd.	R_1	Binding Affinity to Menin IC_{50} (nM)[a]	Cell growth inhibition IC_{50} (nM)[b]	
			MV4;11	MOLM13
7	-CN	6.9 ± 0.4	798 ± 67	870 ± 224
8		4.0 ± 0.3	192 ± 23	553 ± 226
9		1.7 ± 0.4	178 ± 3	703 ± 150
10		3.5 ± 1.2	105 ± 11	274 ± 36
11		2.8 ± 0.2	516 ± 101	599 ± 119
12		3.4 ± 0.2	681 ± 165	675 ± 157
13	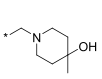	3.5 ± 0.8	421 ± 40	684 ± 240

[a]IC_{50} values were determined using an FP-based competitive binding assay from at least three independent experiments. [b]Cell viability was determined using a CellTiter-Glo Luminescent Cell Viability Assay after 4 days of treatment for each compound, with average values and SDs calculated from three independent experiments.

https://doi.org/10.1021/acs.jmedchem.1c00789
J. Med. Chem. 2021, 64, 10333−10349

with IC_{50} values of 192 and 553 nM in the MV4;11 and MOLM-13 cell lines, respectively. Dimethylation of the primary amine group in **8** led to compound **9**, which binds to menin with an IC_{50} value of 1.7 nM and displays IC_{50} values of 178 nM for MV4;11 cells and 703 nM for MOLM-13 cells. Replacing the dimethylamino group with an azetidine group yielded compound **10**, which binds to menin with an IC_{50} value of 3.5 nM and achieves IC_{50} values of 105 and 274 nM in the MV4;11 and MOLM-13 cell lines, respectively. Expanding the 4-membered ring in compound **10** to a 5-membered ring generated compound **11**, which resulted in an IC_{50} value of 2.8 nM for menin binding and antiproliferative activities for MV4;11 and MOLM-13 cell lines with IC_{50} values of 516 and 599 nM, respectively. Next, we synthesized compounds **12** and **13**, both of which contain a 6-membered ring. Compounds **12** and **13** have binding affinity and cell growth inhibitory activity similar to compound **11**. Based upon the antiproliferative activity in both MV4;11 and MOLM-13 cell lines, compound **10** is the most potent noncovalent inhibitor among the tested compounds shown in Table 1.

We then evaluated the pharmacokinetic (PK) properties of compound **10**, when dosed orally at 25 mg/kg in mice (for details, see the Supporting Information). We found that compound **10** achieves an encouraging oral exposure with average plasma concentrations of 624, 735, and 928 ng/mL at 1, 3, and 6 h post-dosing, respectively.

We next modified the "linker" region in compound **10** to further improve oral exposure while retaining its antiproliferative activity in the MV4;11 and MOLM-13 cell lines. We reasoned that different R_2 groups on the bridge atom of the azetidine will affect the pK_a of the nitrogen atom of the piperidine. This in turn could have a significant effect on the binding affinity to menin and antiproliferative activity in MLL cell lines, as well as on the PK of the resulting compounds. Accordingly, we synthesized and evaluated several analogues of compound **10** with different groups on the bridge atom of the azetidine. These results are summarized in Table 2.

Introduction of a bridge fluorine atom in **10** yielded compound **14**, which shows an IC_{50} value of 3.2 nM for binding to menin and inhibits cell growth in the MV4;11 and MOLM-13 cell lines with IC_{50} values of 222 and 948 nM, respectively. Adding a bridge methyl group in **10** generated compound **15**, which binds to menin with an IC_{50} value of 2.9 nM. Compound **15** has antiproliferative activity in the MV4;11 and MOLM-13 cell lines with IC_{50} values of 272 and 544 nM, respectively. Introduction of a bridge hydroxyl or methoxyl group at the same bridge carbon in **10** resulted in compounds **16** and **17**, which bind to menin with IC_{50} values of 3.6 and 2.5 nM, respectively. Compound **16** has IC_{50} values of 379 nM in MV4;11 cells and 833 nM in the MOLM-13 cell line, while compound **17** is about 2-fold more potent than **16**. Addition of a bridging methyl ester group to **10** led to compound **18**, which is more than 10-fold less potent than **10** in its binding affinity to menin. Consistent with its lower binding affinity, compound **18** has a weak cell growth inhibitory activity in both the MV4;11 and MOML-13 cell lines. Hence, among these analogues with a substituted bridging atom, compound **17** with a bridging methoxyl group is the most potent compound based upon its cell growth inhibitory activity in both the MV4;11 and MOLM-13 cell lines.

We then evaluated the oral exposure of compound **17** in mice. A single oral administration of compound **17** at 25 mg/kg achieves average plasma compound concentrations of 8265, 5750, and 2195 ng/mL at 1, 3, and 6 h post-dosing, respectively. Hence, while compound **17** is slightly less potent than compound **10** in inhibiting cell growth in both the MV4;11 and MOLM-13 cell lines, **17** displays much improved oral plasma exposure when compared to **10** in mice.

Design of Covalent Inhibitors Based upon Compound 17. These promising cellular and oral exposure data for compound **17** prompted us to design and synthesize a series of covalent menin inhibitors based on this noncovalent inhibitor with the objective of improving cellular potency in MLLr cell lines. We tested these covalent inhibitors for their binding affinities to menin by the FP-based assay and their antiproliferative activities in the MV4;11 and MOLM-13 cell lines. These results are summarized in Table 3.

We replaced the cyclopropyl group in **17** with the Michael acceptor used in M-525 to obtain compound **19**. Compound **19** shows improved antiproliferative activity with IC_{50} values of 2.3 and 49 nM in MV4;11 and MOLM-13 cell lines, respectively. Compound **19** thus is 72- and 9-fold more potent than compound **17** in inhibiting proliferation of MV4;11 and MOLM-13 cell lines, respectively, suggesting that compound **19** behaves as a covalent menin inhibitor in cells.

In both M-525 and M-808, a positively charged group was attached to the Michael acceptor. Our data show that the positively charged group in M-525 and M-808 is critical in increasing the reactivity of the Michael acceptor for rapid formation of a covalent bond with menin, and such enhanced reactivity leads to improved antiproliferative activity in MLLr leukemia cells.[26,28] However, we hypothesized that the positively charged group attached to the Michael acceptor in M-525 and M-808 molecules diminishes the oral bioavailability of these compounds. Therefore, we decided to synthesize and test a series of potential covalent menin inhibitors lacking the positively charged group attached to the Michael acceptor.

Removal of the positively charged group attached to the Michael acceptor in compound **19** yielded compound **20**. As expected and consistent with our previous data, compound **20** is 49- and 8-fold less potent than compound **19** in inhibiting growth of MV4;11 and MOLM-13 cell lines, respectively. Therefore, while compounds **19** and **20** contain the same acrylamide Michael acceptor, compound **20** has a much weaker cell growth inhibitory potency in both the MV4;11 and

Table 2. Binding Affinity and Cell Growth Inhibition Values of Menin Inhibitors (14−18)[a]

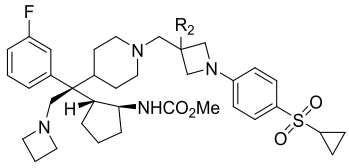

compd.	R_2	binding affinity to menin IC_{50} (nM)	cell growth inhibition (nM) MV4;11	MOLM13
10	−H	3.5 ± 1.2	105 ± 11	274 ± 36
14	−F	3.2 ± 0.2	222 ± 31	948 ± 305
15	−Me	2.9 ± 0.5	272 ± 17	544 ± 145
16	−OH	3.6 ± 0.8	379 ± 54	833 ± 179
17	−OMe	2.5 ± 0.3	166 ± 9	443 ± 120
18	−COOMe	42.4 ± 4.0	>1000	>10,000

[a] IC_{50} values are averages of three independent experiments.

https://doi.org/10.1021/acs.jmedchem.1c00789
J. Med. Chem. 2021, 64, 10333−10349

Table 3. Binding Affinity and Cell Growth Inhibition Values of Menin Inhibitors 19-26[a]

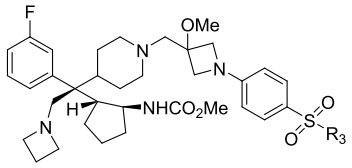

Compd.	R_3	Binding affinity to menin (IC_{50} (nM))	Cell growth inhibition (IC_{50} (nM))	
			MV4;11	MOLM13
19	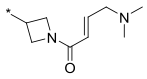	2.7±0.5	2.3 ± 0.7	49.7 ± 7.2
20		2.8±0.3	112 ± 33	402 ± 246
21	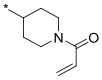	3.8 ± 0.5	156 ± 30	594 ± 195
22	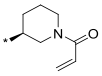	3.0 ± 0.4	77 ± 15	196 ± 44
23	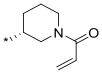	3.7 ± 0.3	74 ± 24	188 ± 8
24 (M-1121)	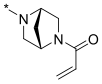	2.7 ± 0.1	10.3 ± 2.9	51.5 ± 13.5
25	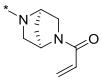	4.6 ± 1.7	436 ± 89	504 ± 42
26	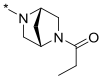	4.2 ± 0.7	289 ± 82	630 ± 192

[a]IC_{50} values are averages of three independent experiments.

MOLM-13 cell lines, indicating that compound **20** probably does not form a covalent bond with menin very efficiently in cells.

We reasoned that the Michael acceptor in compound **20** may not able to adopt an optimal position and/or orientation for efficient formation of a covalent bond with menin upon binding. Therefore, we synthesized compounds **21**−**23** with different conformationally constrained linking groups between the SO_2 group and the acrylamide to determine if other linkers would place the Michael acceptor in a more optimal position and orientation for efficient covalent bond formation with menin protein.

Compound **21** employing a 6-membered ring piperidine linker is slightly less potent than compound **20** in cell growth inhibition in the MV4;11 and MOLM-13 cell lines. Changing the acrylamide from the 4-position in compound **21** to the 3-position in the piperidine linker with either an (*S*)- or (*R*)-configuration generated compounds **22** and **23**, respectively. Compounds **22** and **23** are both 2 times more potent than compound **21** in the MV4;11 and MOLM-13 cell lines and marginally more potent than compound **20** in both cell lines. Since compounds **21**−**23** are all much less potent than compound **19**, these compounds are still likely incapable of efficiently forming a covalent bond with menin in cells.

We hypothesized that further conformational restriction of the linker may lock the acrylamide Michael acceptor group in an optimal position and orientation for efficient formation of a covalent bond with the thiol group of Cys329 in menin. Computational modeling suggested that a highly conformationally constrained (1*S*,4*S*)-2,5-diazabicyclo[2.2.1]heptane linker would lock the acrylamide in an optimal position and orientation for efficient formation of a covalent bond with the thiol group of Cys 329 (Supporting Information). Interestingly, the enantiomer (1*R*,4*R*)-2,5-diazabicyclo[2.2.1]heptane linker was predicted to place the acrylamide much further away (4.7 Å) from the thiol group of the Cys 329 residue, suggesting that a formation of a covalent bond is unlikely.

To test our predictions, we synthesized compounds **24** and **25** using these two enantiomeric 2,5-diazabicyclo[2.2.1]-heptane linkers. Consistent with our predictions, compound **24** containing the (1*S*,4*S*)-2,5-diazabicyclo[2.2.1]heptane linker is a very potent inhibitor with IC_{50} values of 10.3 and 51.5 nM in the MV4;11 and MOLM-13 cell lines. In comparison, the stereoisomer compound **25** containing the (1*R*,4*R*)-2,5-diazabicyclo[2.2.1]heptane is a much weaker inhibitor and displays IC_{50} values of 436 and 504 nM in the MV4;11 and MOLM-13 cell lines, respectively. Hence, compound **24**, which was named M-1121, is 40- and 9-fold more potent than its stereoisomer compound **25** in the MV4;11 and MOLM-13 cell lines, respectively. These data show that the stereochemistry of the linker in M-1121 is critically important for its potent activity in MLLr leukemia cells. M-1121 is also 8−10-fold more potent than compound **20** in both MV4;11 and MOLM-13 cell lines.

We synthesized compound **26** by converting the acrylamide in compound **24** into propionamide to further test the importance of covalent bond formation for cell growth inhibition (Table 3). Compound **26** is >10 times less potent than **24** in inhibition of cell growth in MV4;11 and MOLM-13 cell lines (Table 3), highlighting the importance of covalent formation for achieving high cellular potency in MLLr leukemia cell lines.

To gain further insights into their mode of action and cellular activity, we analyzed compounds **19**−**26** for covalent complex formation with recombinant human menin protein by mass spectrometry using four different incubation times (10, 30, 60 min, and overnight) and obtained the data summarized in Table 4.

In general, the reaction kinetic data for compounds **19**−**26** with menin protein (Table 4) correlate nicely with their potencies in inhibition of cell growth in both MV4;11 and MOLM-13 cell lines (Table 3). Compound **19** is the most potent inhibitor in cell growth inhibition and has the fastest kinetics in formation of a covalent complex with menin protein among compounds **19**−**26**. With 10, 30, 60 min, and overnight incubation times, 36.9, 83.4, 85.4, and 90.9% of menin protein form a covalent complex with compound **19**, respectively. M-1121 has the second fastest kinetics in formation of a covalent complex with menin protein and is also the second most potent inhibitor. This is followed by compound **20** as the third most potent compound with the third fastest kinetics. Compounds **22** and **23** have a slower reaction kinetics than compounds **19**, **20**, and M-1121, consistent with their weaker cellular activities than compounds **19**, **20**, and M-1121.

https://doi.org/10.1021/acs.jmedchem.1c00789
J. Med. Chem. 2021, 64, 10333−10349

Table 4. Analysis of Covalent Complex Formation of Menin Inhibitors with Recombinant Human Menin Protein by Mass Spectrometry

	incubation time with menin protein			
	10 min	30 min	1 h	overnight
compound	% of menin covalent complex			
19	36.9%	83.4%	85.4%	90.9%
20	24.1%	40.9%	59.4%	81.5%
21	0%	0%	0%	27.0%
22	8.8%	27.9%	37.4%	93.1%
23	9.8%	22.6%	40.5%	90.0%
24 (M-1121)	27%	59%	66%	100%
25	0%	0%	0%	45.1%
26	0%	0%	0%	0%

Compounds **21** and **25** have a very slow reaction kinetics, and no covalent complex was detected within 1 h incubation time. Consistent with its lack of a Michael acceptor, compound **26** does not form a covalent complex with menin even with overnight incubation. Of note, the stoichiometry for each inhibitor:menin covalent complex was 1:1.2.

A glutathione (GSH) reactivity assay was employed to test the intrinsic reactivity of M-1121 toward glutathione (GSH). Incubation of M-1121 under conditions mimicking intracellular glutathione levels (4.5 mM GSH, 37 °C, pH 7.4) revealed a GSH conjugation half-life of 89 min. These data indicated that M-1121 has only mild reactivity with GSH.

To further understand the precise binding mode, we determined the co-crystal structure for M-1121 in complex with menin at 2.74 Å resolution (Figure 2.). Consistent with our design and mass spectrometry data, M-1121 forms a covalent bond between the acrylamide Michael acceptor and the thiol group of Cys329 in menin. The 2,5-diazabicyclo [2.2.1] ring orients and places the acrylamide group in a position that is optimal for the formation of a covalent bond with the sulfur atom in the Cys329 of menin. In addition, the 2,5-diazabicyclo [2.2.1] group establishes hydrophobic interactions with menin, specifically with Val371, Ala325, and Gly326. The nitrogen atom of the azetidine head group is 4.1 Å from the negatively charged carboxylic acid group of the Asp180 side chain in menin, indicating a charge−charge interaction. The methoxy group on the azetidine linker in M-1121 forms a hydrogen bond with the phenol group of Tyr323.

M-1121 was evaluated for its antiproliferative activity in 4 MLLr and 3 MLL wild-type cell lines to further define its cellular activity and selectivity. We found that M-1121 potently inhibits proliferation of MLL rearranged but not MLL wild-type cell lines up to 10 μM, highlighting the selective activity of M-1121 for cells carrying MLL translocations (Table 5).

Table 5. Cell Growth Inhibitory Activities of M-1121 in a Panel of Leukemia Cell Lines after 4 Days of Treatment Determined by the CellTiter-Glo

cell line[a]	MLL status	disease indication	cell growth inhibition IC_{50} (nM)
MV4;11	MLL/AF4	ALL	10
MOLM-13	MLL/AF9	AML	52
OCI-AML4	MLL-ENL	AML	3
SEM	MLL/AF4	ALL	51
KOPN8	MLL/ENL	ALL	110
RS4;11	MLL/AF4	ALL	1000
HL-60	MLLwt	AML	>10,000
K562	MLLwt	CML	>10,000
MEG-1	MLLwt	CML	>10,000

[a]AML: acute myeloid leukemia; ALL: acute lymphocytic leukemia; CML: chronic myeloid leukemia.

In our previous studies, we showed that menin inhibitors suppress the expression of *HOXA9* and *MEIS1* in MLLr leukemia cells.[24,28] We thus evaluated M-1121 for its effect on the expression of *HOXA9* and *MEIS1* in MV4;11 cells by qRT-PCR. Our data showed that M-1121 suppresses *HOXA9* and *MEIS1* gene transcription in a dose-dependent manner and effectively modulates the expression of *HOXA9* and *MEIS1* genes at concentrations as low as 10 and 30 nM, respectively (Figure 3). Hence, M-1121 is potent in inhibiting the expression of *HOXA9* and *MEIS1* gene transcription in the

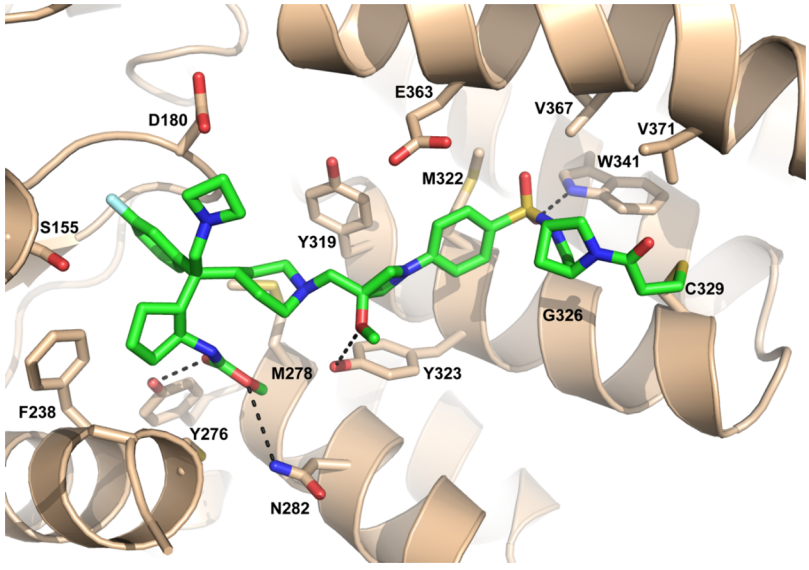

Figure 2. Co-crystal structure of compound **24** (M-1121) complexed with menin at 2.74 Å resolution (PDB code: 7M4T). Side chains of menin residues within 4 Å from the compound are shown as sticks. Hydrogen bonds are shown as dashed lines.

https://doi.org/10.1021/acs.jmedchem.1c00789
J. Med. Chem. 2021, 64, 10333−10349

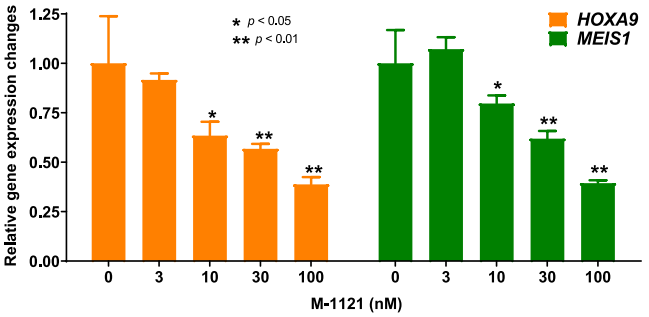

Figure 3. Gene expression changes induced by M-1121. Quantitative real-time polymerase chain reaction (qRT-PCR) analysis of the effect of M-1121 on the mRNA levels of *HOXA9* and *MEIS1*genes in MV4;11 cells after 24 h of treatment.

M4;11 cell line, consistent with the expected mechanism of action of a menin inhibitor.

Next, we evaluated the oral exposure of M-1121 in mice. A single oral administration of M-1121 at 25 mg/kg achieves average plasma concentrations of 3797, 4640, and 2055 ng/mL at 1, 3, and 6 h post-dosing, respectively, indicating excellent oral exposure. Subsequently, a PK study with both intravenous and oral administrations was performed with M-1121. The PK data showed that M-1121 has a low clearance and a moderate volume of distribution (Table 6). M-1121 dosed orally at 5 mg/kg achieves a C_{max} value of 4153 ng/mL and $AUC_{0-\infty}$ of 43,567 h·ng/mL. Together, M-1121 has an acceptable PK profile in mice with 49.4% oral bioavailability.

We determined the plasma protein binding data for M-1121 and found that M-1121 has 90.7, 87.5, and 99.3% binding in human, rat, and mouse plasma, respectively. The PPB data showed that while M-1121 has an excellent PPB in human and rat plasma, it has a very high PPB in mouse plasma, suggesting that high doses may be needed to achieve strong antitumor activity in mice.

We next evaluated M-1121 for its *in vivo* antitumor activity in SCID mice harboring MV4;11 subcutaneous tumors. In the first experiment, when xenograft tumors reached an average volume of 100 mm^3, mice were treated with M-1121 at 100 mg/kg daily for 26 days *via* oral gavage (Figure 4a,b). M-1121 reduced the average tumor volume from 157 mm^3 at the beginning of the treatment to 106 mm^3 on day 26 of the treatment, a reduction of tumor volume of 32%. Significantly, M-1121 caused no animal weight loss or other signs of toxicity during and after the treatment.

Because of the high PPB (99.3%) of M-1121 in mouse plasma and importantly its lack of any signs of toxicity in mice at 100 mg/kg, we further tested its antitumor activity in the MV4;11 subcutaneous tumor model at a higher dose to determine if M-1121 can achieve an even stronger antitumor activity. In the second experiment, when tumors reached an average volume of 200 mm^3, mice were treated with M-1121 at 300 mg/kg once daily for 15 days *via* oral gavage (Figure 4c,d). M-1121 led to complete tumor regression in 10 out of 10 mice with no tumor regrowth detected up to a month after last treatment (day 45 after treatment start) (Figure 4c and Figure S2 in the Supporting Information). Treatment with M-1121 was well tolerated with no significant body weight loss (Figure 4d) or other signs of toxicity.

Since MLLr leukemias are bone marrow diseases, we next investigated whether M-1121 has activity in this compartment by evaluating the effect of M-1121 in bone marrow $CD45^+$ leukemic cells in NCG mice engrafted with the Luciferase-tagged MV4;11 disseminated model. Mice were dosed with M-1121 at 150 mg/kg once daily by oral gavage for 4 days to achieve steady-state drug levels, and we evaluated the effect at a 48 h time-point post-last dose. We found that M-1121 suppresses the expression of the MEIS1 gene to less than 2% compared to the vehicle group with concomitant induction of the cell differentiation marker ITGAM (~67-fold) and CD11b protein in human $CD45^+$ cells isolated from bone marrow (Figure 5a,b). It is interesting to note that even though mice were treated for only 4 days, M-1121 was able to exert antitumor activity with reduction in the number of human $CD45^+$ $CD33^+$ leukemic cells in bone marrow as detected by flow cytometry (Figure 5c) and decrease the intensity of the whole-body bioluminescence signal (Figure 5d). No significant changes in body weight were observed (data not shown).

Chemistry. The synthetic routes to these compounds are shown below (Scheme 1). Compounds **8**−**13** were synthesized in a convergent manner. The Boc group in the known compound **27**[28] was deprotected with TFA, and the resulting amine was converted into a methyl carbamate **28**. A relay reduction of **28** with DIBAL-H followed by $NaBH_4$ was employed to give primary amine **29**, which was subjected to Boc protection. Removal of the benzyl protecting group followed by substitution and removal of the Boc group afforded compound **8**, whose subsequent functionalization gave **9**−**13**. Intermediate **36** was synthesized in five steps starting from 4-fluorobenzenethiol.

Synthesis of compounds **14**−**18** (Scheme 2) started with compound **29**. A ring-closure/substitution reaction gave an azetidine compound **37**. Removal of the benzyl protecting group followed by substitution with **41** afforded compound **39**. Then the Boc group was cleaved, and the resulting product was submitted to a nucleophilic aromatic substitution reaction with **34** to give **14**−**18** as the final compounds.

Starting from **39d**, compounds **19**−**26** were synthesized in a similar manner (Scheme 3). Removal of Boc protection from **39d** followed by aromatic substitution with **42** gave compound **40**. Removal of the Boc protection from **40** produced the corresponding amine intermediates, which reacted with diverse carbonyl chlorides or anhydrides to afford the final products **19**−**26**.

Table 6. Pharmacokinetics of M-1121 in Mice[a]

	1 mg/kg (IV)			5 mg/kg (PO)			
compd.	CL (L/h/kg)	*Vss* (L/kg)	$AUC_{0-\infty}$ (h·ng/mL)	t_{max} (h)	C_{max} (ng/mL)	$AUC_{0-\infty}$ (h·ng/mL)	*F*%
M-1121	0.0567	0.330	17,644	2.00	4153	43,567	49.4

[a]Female C57BL/6 mice were dosed either intravenously with a solution in 10% NMP, 10% Solutol HS15, and 80% saline or orally at 5 mg/kg in 0.5% methyl cellulose + 0.2% Tween 80 (w/w).

https://doi.org/10.1021/acs.jmedchem.1c00789
J. Med. Chem. 2021, 64, 10333−10349

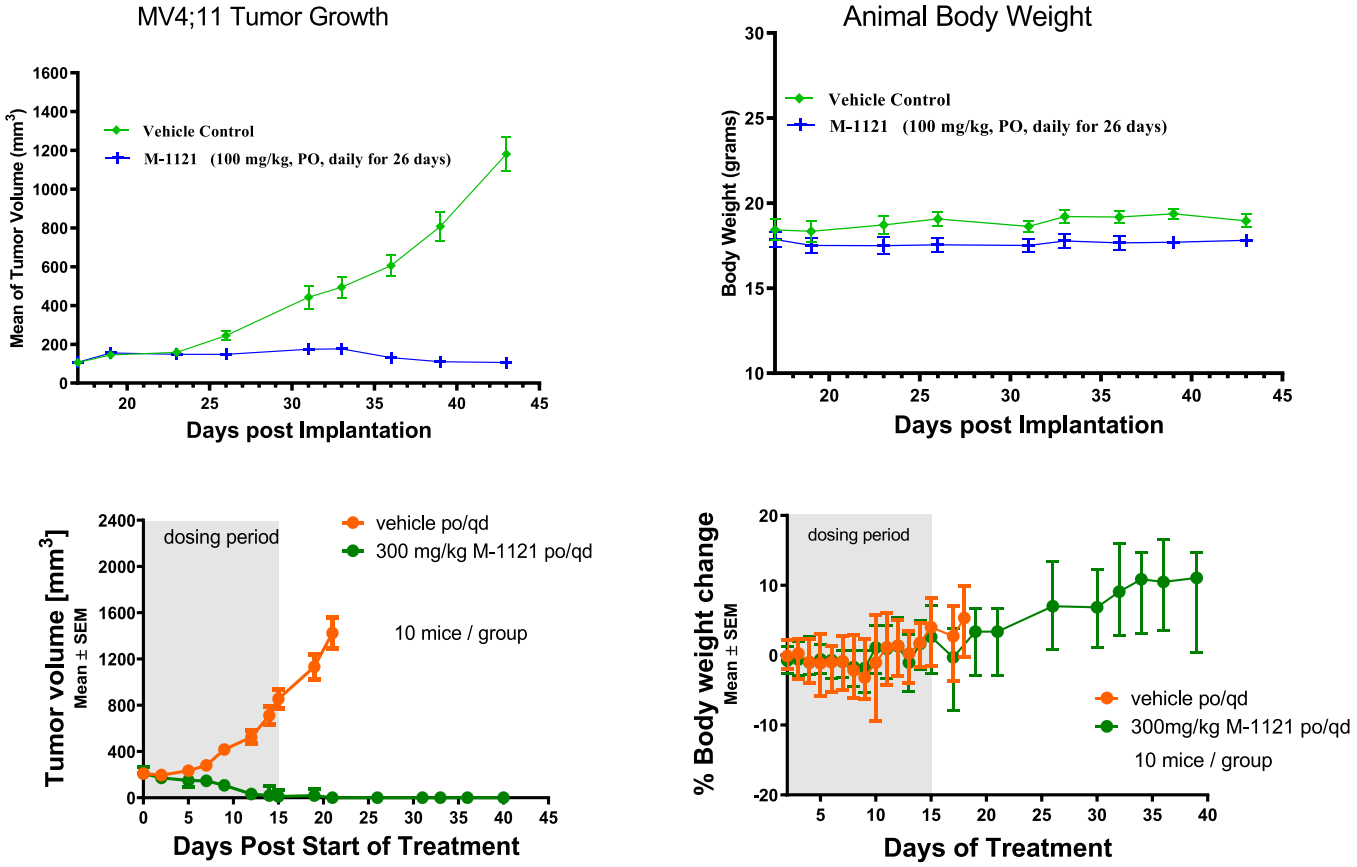

Figure 4. M-1121 exhibits potent antitumor efficacy in the MV4;11 (MLL rearranged) subcutaneous tumor xenograft model. The compound was administered orally at the indicated dose schedules.

EXPERIMENTAL SECTION

General Methods for Chemistry. Unless otherwise noted, commercial solvents and reagents were used without further purification. Proton nuclear magnetic resonance (^{1}H NMR) spectra were recorded on a Bruker Advance 400 MHz spectrometer and are reported in parts per million (ppm) downfield from tetramethylsilane (TMS). In the spectral data reported, the format (δ) chemical shift (multiplicity, J values in Hz, integration) was used with the following abbreviations: s = singlet, d = doublet, t = triplet, q = quartet, and m = multiplet. Mass spectrometric (MS) analysis was carried out with a Waters ultraperformance liquid chromatography (UPLC)−mass spectrometer. The final compounds were all purified by a C18 reversed-phase preparative high-performance liquid chromatography (HPLC) column with solvent A (0.1% TFA in H_2O) and solvent B (0.1% TFA in MeCN). The purity of all the final compounds was confirmed to be >95% by UPLC analysis (10−100% MeCN in H_2O containing 0.1% TFA in 10 min).

*Methyl ((1S,2R)-2-((S)-Cyano(1-((1-(4-(cyclopropylsulfonyl)-phenyl)azetidin-3-yl)methyl)piperidin-4-yl)(3-fluorophenyl)-methyl)cyclopentyl)carbamate (**7**).* Compound **7** was prepared from compounds **28** and **36** with the procedure that was used to produce compound **31**. ^{1}H NMR (400 MHz, MeOH-d4) δ 7.49−7.44 (m, 2H), 7.25 (td, J = 8.1, 6.1 Hz, 1H), 7.15 (d, J = 7.9 Hz, 1H), 7.07 (d, J = 10.2 Hz, 1H), 6.98−6.92 (m, 1H), 6.36−6.26 (m, 2H), 3.95 (td, J = 8.0, 2.0 Hz, 2H), 3.68 (q, J = 6.8 Hz, 1H), 3.53 (dd, J = 8.1, 5.6 Hz, 2H), 3.38 (t, J = 11.6 Hz, 1H), 3.25 (s, 1H), 3.23 (s, 3H), 3.13 (p, J = 1.6 Hz, 1H), 3.08−2.94 (m, 1H), 2.92−2.79 (m, 2H), 2.67 (q, J = 7.9 Hz, 1H), 2.37 (tt, J = 7.9, 4.8 Hz, 1H), 2.26 (t, J = 12.1 Hz, 1H), 2.10−1.91 (m, 2H), 1.83−1.75 (m, 1H), 1.70−1.59 (m, 1H), 1.58−1.31 (m, 5H), 1.29−1.13 (m, 1H), 1.00−0.93 (m, 2H), 0.84−0.77 (m, 2H); ESI-MS calcd for $C_{33}H_{42}FN_4O_4S$ $[M + H]^+$ = 609.29, found: 609.14.

*Methyl ((1S,2R)-2-((S)-2-Amino-1-(1-((1-(4-(cyclopropylsulfonyl)-phenyl)azetidin-3-yl)methyl)piperidin-4-yl)-1-(3-fluorophenyl)-ethyl)cyclopentyl)carbamate (**8**).* Compound **31** (680 mg, 0.954 mmol) was dissolved in DCM (3 mL), and TFA (1.5 mL) was added slowly. After stirring for 3 h at room temperature (rt), the reaction mixture was concentrated under vacuum. The residue was purified with preparative HPLC to give the title compound (495 mg, 85%). ^{1}H NMR (400 MHz, MeOH-d4) δ 7.64−7.59 (m, 2H), 7.44 (q, J = 7.6 Hz, 1H), 7.24−7.16 (m, 2H), 7.13 (t, J = 8.8 Hz, 1H), 6.77−6.71 (m, 2H), 3.81−3.66 (m, 4H), 3.66−3.53 (m, 2H), 3.53−3.45 (m, 1H), 3.31−3.20 (m, 4H), 3.20−3.09 (m, 3H), 3.02 (t, J = 12.3 Hz, 1H), 2.93 (t, J = 12.5 Hz, 1H), 2.89−2.70 (m, 2H), 2.57 (m, 1H), 2.41 (s, 1H), 2.18−2.08 (m, 1H), 2.04−1.94 (m, 3H), 1.94−1.82 (m, 1H), 1.82−1.67 (m, 2H), 1.67−1.54 (m, 3H), 1.21−1.12 (m, 2H), 1.06−0.97 (m, 2H); ESI-MS calcd for $C_{33}H_{46}FN_4O_4S$ $[M + H]^+$ = 613.32, found: 613.17.

*Methyl ((1S,2R)-2-((S)-1-(1-((1-(4-(Cyclopropylsulfonyl)phenyl)-azetidin-3-yl)methyl)piperidin-4-yl)-2-(dimethylamino)-1-(3-fluorophenyl)ethyl)cyclopentyl)carbamate (**9**).* Triethylamine (23 μL, 0.163 mmol), acetic acid (15 μL, 0.261 mmol), and formaldehyde (3 μL, 0.196 mmol) were added to a solution of compound **8** (40 mg, 0.0653 mmol) in MeCN/THF (0.5/0.5 mL). After 3 h, sodium triacetoxyborohydride (42 mg, 0.196 mmol) was added. The mixture was stirred overnight, quenched with H_2O, and concentrated under vacuum. The residue was purified by reversed-phase preparative HPLC to give the title compound (22 mg, 53%). ^{1}H NMR (400 MHz, MeOH-d4) δ 7.71−7.66 (m, 2H), 7.56−7.48 (m, 1H), 7.46−7.37 (m, 2H), 7.21−7.14 (m, 1H), 6.58−6.51 (m, 2H), 4.21 (t, J = 8.0 Hz, 2H), 4.01−3.83 (m, 3H), 3.79 (ddd, J = 8.3, 5.6, 2.9 Hz, 2H), 3.72−3.59 (m, 2H), 3.57−3.43 (m, 4H), 3.31−3.19 (m, 2H), 3.16−3.01 (m, 3H), 3.01−2.82 (m, 4H), 2.69 (d, J = 7.4 Hz, 1H), 2.58 (tt, J = 8.0, 4.8 Hz, 1H), 2.44 (s, 1H), 2.28−2.11 (m, 2H), 2.06−1.93 (m, 1H), 1.70 (m, 3H), 1.60 (m, 3H), 1.42 (m, 1H), 1.33 (t, J = 7.3 Hz,

https://doi.org/10.1021/acs.jmedchem.1c00789
J. Med. Chem. 2021, 64, 10333−10349

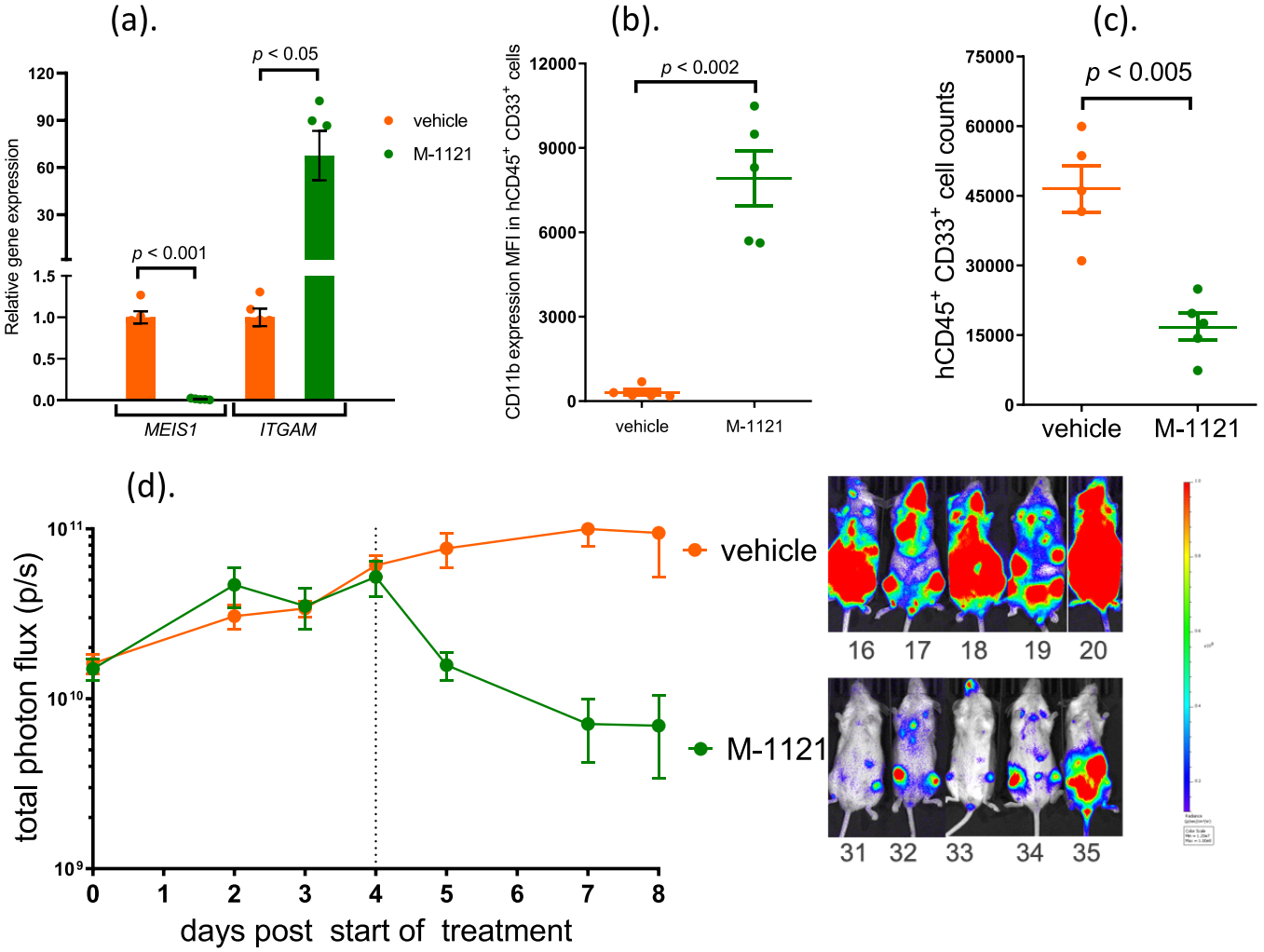

Figure 5. M-1121 shows activity in the disseminated Luciferase-tagged MV4;11 (MLL rearranged) xenograft model. M-1121 was administered *via* oral gavage at 150 mg/kg once daily for 4 days, and data are presented as mean ± SEM, and five mice were evaluated per group. Readouts in a, b, and c were measured 48 h after the last dose. *MEIS1* and *ITGAM* gene expression in human $CD45^+$ cells isolated from bone marrow evaluated by RT-qPCR (a), CD11b mean fluorescence intensity (MFI) measured in human $CD45^+$ $CD33^+$ cells from bone marrow by flow cytometry (b), the number of human $CD45^+$ $CD33^+$ cells measured by flow cytometry (c) and whole-body bioluminescence intensity determined in vehicle or M-1121-treated mice (d). The dotted line indicates the last day of dosing.

1H), 1.21−1.14 (m, 2H), 1.05−0.98 (m, 2H); ESI-MS calcd for $C_{35}H_{50}FN_4O_4S$ $[M + H]^+$ = 641.35, found: 641.20.

*Methyl ((1S,2R)-2-((S)-2-(Azetidin-1-yl)-1-(1-((1-(4-(cyclopropylsulfonyl)phenyl)azetidin-3-yl)methyl)piperidin-4-yl)-1-(3-fluorophenyl)ethyl)cyclopentyl)carbamate (**10**).* 1,3-Dibromopropane (8 μL, 0.0784 mmol), K_2CO_3 (27 mg, 0.196 mmol), and KI (1 mg, 0.00653 mmol) were added to a solution of compound **8** (40 mg, 0.0653 mmol) in MeCN (1.5 mL). The mixture was stirred at 80 °C overnight, quenched with H_2O, and concentrated under vacuum. The residue was purified by reversed-phase preparative HPLC to give the title compound (26 mg, 61%). ^{1}H NMR (400 MHz, MeOH-d4) δ 7.69−7.63 (m, 2H), 7.47 (td, J = 8.1, 6.2 Hz, 1H), 7.19−7.11 (m, 2H), 7.06 (d, J = 8.0 Hz, 1H), 6.55−6.49 (m, 2H), 4.60−4.46 (m, 2H), 4.42−4.28 (m, 2H), 4.21−4.10 (m, 3H), 3.79 (d, J = 15.6 Hz, 1H), 3.72 (ddd, J = 8.0, 5.6, 2.4 Hz, 2H), 3.61−3.44 (m, 3H), 3.41 (d, J = 7.1 Hz, 2H), 3.26−3.16 (m, 1H), 2.99 (dt, J = 24.9, 12.4 Hz, 2H), 2.79 (d, J = 9.4 Hz, 1H), 2.57 (tt, J = 7.9, 4.8 Hz, 2H), 2.50−2.39 (m, 1H), 2.13−1.96 (m, 5H), 1.93−1.83 (m, 1H), 1.83−1.74 (m, 1H), 1.73−1.57 (m, 3H), 1.47 (q, J = 12.9 Hz, 1H), 1.19−1.12 (m, 2H), 1.04−0.96 (m, 2H); ESI-MS calcd for $C_{36}H_{50}FN_4O_4S$ $[M + H]^+$ = 653.35, found: 653.10.

*Methyl ((1S,2R)-2-((S)-1-(1-((1-(4-(Cyclopropylsulfonyl)phenyl)-azetidin-3-yl)methyl)piperidin-4-yl)-1-(3-fluorophenyl)-2-(pyrrolidin-1-yl)ethyl)cyclopentyl)carbamate (**11**).* Compound **11** was prepared from compound **8** and 1,4-dibromobutane according to the procedure used to produce compound **10** (26 mg, 60%). ^{1}H NMR (400 MHz, MeOH-d4) δ 7.71−7.65 (m, 2H), 7.49 (td, J = 8.0, 6.3 Hz, 1H), 7.39−7.30 (m, 2H), 7.20−7.12 (m, 1H), 6.56−6.50 (m, 2H), 4.17 (t, J = 8.0 Hz, 2H), 3.91−3.67 (m, 6H), 3.64−3.50 (m, 3H), 3.49−3.40 (m, 3H), 3.38−3.35 (m, 2H), 3.29−3.18 (m, 2H), 3.05 (t, J = 12.4 Hz, 1H), 2.96 (t, J = 12.5 Hz, 1H), 2.90−2.77 (m, 1H), 2.58 (tt, J = 7.9, 4.8 Hz, 1H), 2.32−1.98 (m, 8H), 1.98−1.86 (m, 1H), 1.86−1.49 (m, 6H), 1.44−1.25 (m, 1H), 1.20−1.13 (m, 2H), 1.06−0.97 (m, 2H); ESI-MS calcd for $C_{37}H_{52}FN_4O_4S$ $[M + H]^+$ = 667.37, found: 667.25.

*Methyl ((1S,2R)-2-((S)-1-(1-((1-(4-(Cyclopropylsulfonyl)phenyl)-azetidin-3-yl)methyl)piperidin-4-yl)-1-(3-fluorophenyl)-2-morpholinoethyl)cyclopentyl)carbamate (**12**).* Compound **12** was prepared from compound **8** and bis(2-bromoethyl) ether according to the procedure used to prepare compound **10** (20 mg, 45%). ^{1}H NMR (400 MHz, MeOH-d4) δ 7.70−7.64 (m, 2H), 7.45 (q, J = 7.6 Hz, 1H), 7.39 (d, J = 9.6 Hz, 2H), 7.17−7.06 (m, 1H), 6.56−6.49 (m, 2H), 4.18 (t, J = 8.0 Hz, 2H), 3.92 (s, 4H), 3.80−3.68 (m, 4H), 3.64−3.52 (m, 4H), 3.49−3.36 (m, 6H), 3.29−3.10 (m, 2H), 3.04 (t, J = 12.5 Hz, 1H), 2.92 (t, J = 12.4 Hz, 1H), 2.81 (s, 1H), 2.58 (tt, J = 7.9, 4.8 Hz, 1H), 2.24−2.07 (m, 3H), 2.07−1.93 (m, 2H), 1.70 (s,

https://doi.org/10.1021/acs.jmedchem.1c00789
J. Med. Chem. 2021, 64, 10333−10349

Scheme 1. Synthesis of Compounds 8−13[a]

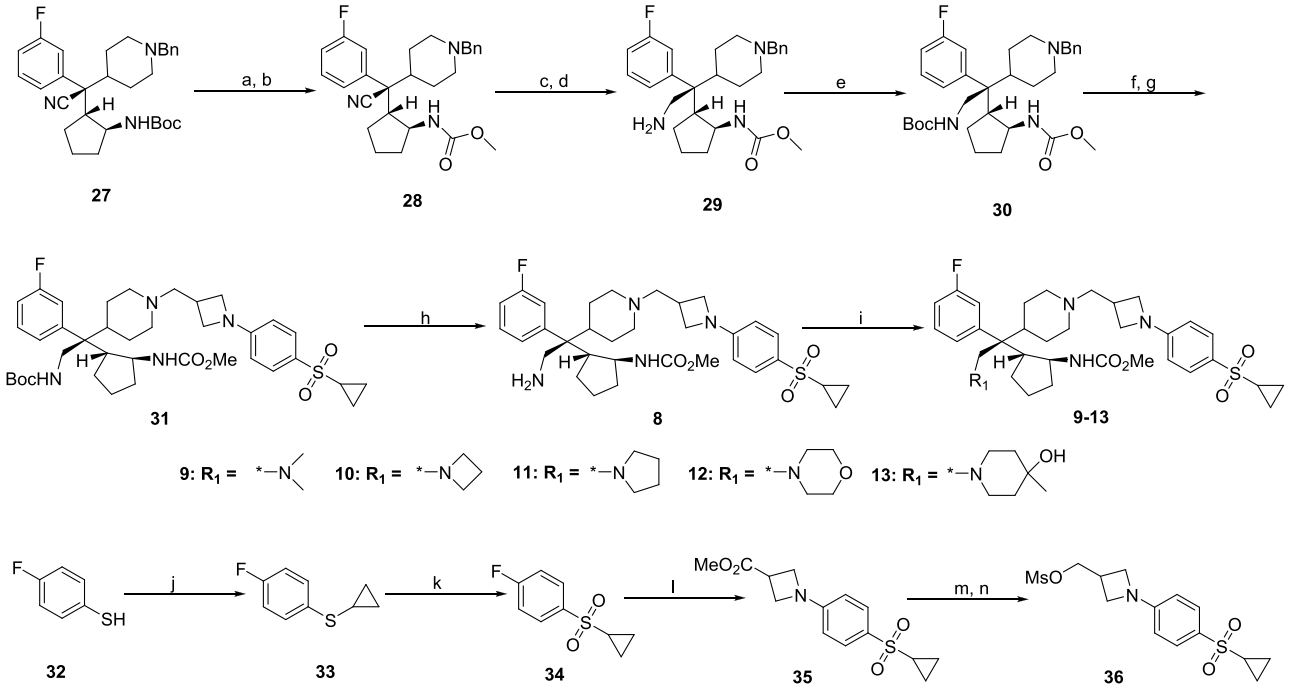

[a]Reagents and conditions: (a) TFA, DCM, rt; (b) dimethyl dicarbonate, Et_3N, DCM, rt; (c) DIBAL-H, toluene, 0 °C; (d) $NaBH_4$, MeOH, 0 °C to rt; (e) Boc_2O, DCM, rt; (f) H_2, Pd/C, MeOH, rt; (g) **36**, K_2CO_3, KI, MeCN, 80 °C; (h) TFA, DCM, rt; (i) formaldehyde, $NaBH(OAc)_3$, MeCN/THF, rt (**9**); 1,4-dibromobutane, K_2CO_3, MeCN, 80 °C (**10**); 1,5-dibromopentane, K_2CO_3, MeCN, 80 °C (**11**); 1-bromo-2-(2-bromoethoxy)ethane, K_2CO_3, MeCN, 80 °C (**12**); methallyltrimethylsilane, formaldehyde, H_2O, 45 °C (**13**); (j) bromocyclopropane, *t*-BuONa, DMSO, 80 °C; (k) *m*-CPBA, DCM, rt; (l) methyl azetidine-3-carboxylate hydrochloride, K_2CO_3, DMSO, 80 °C; (m) $LiAlH_4$, THF, 0 °C; (n) MsCl, Et_3N, DCM, rt.

Scheme 2. Synthesis of Compounds 14−18[a]

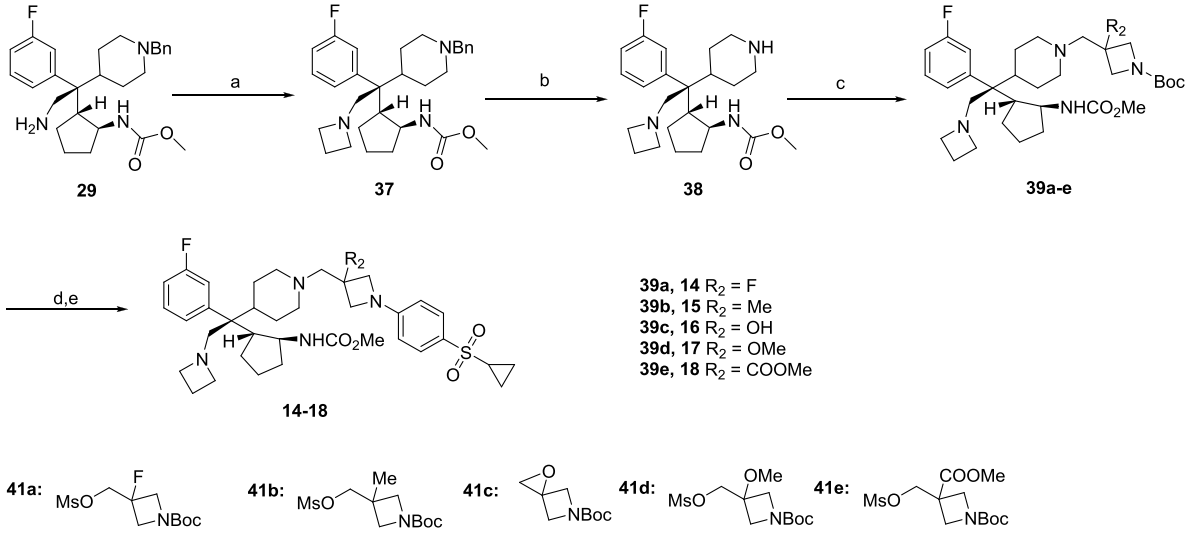

[a]Reagents and conditions: (a) 1,3-dibromopropane, K_2CO_3, KI, MeCN, 80 °C; (b) H_2, Pd/C, MeOH, rt; (c) **41**, K_2CO_3, KI, MeCN, 80 °C; (d) TFA, DCM, rt; (e) **34**, K_2CO_3, DMSO, 80 °C.

7H), 1.20−1.13 (m, 2H), 1.05−0.97 (m, 2H); ESI-MS calcd for $C_{37}H_{52}FN_4O_5S$ $[M + H]^+$ = 683.36, found: 683.23.

Methyl ((1S,2R)-2-((S)-1-(1-((1-(4-(Cyclopropylsulfonyl)phenyl)-azetidin-3-yl)methyl)piperidin-4-yl)-1-(3-fluorophenyl)-2-(4-hydroxy-4-methylpiperidin-1-yl)ethyl)cyclopentyl)carbamate (13). Compound **13** was prepared according to a reported procedure.[29] Methallyltrimethylsilane (32 μL, 0.184 mmol) and formaldehyde (41 μL, 0.488 mmol) were added to a solution of compound **8** (75 mg, 0.1223 mmol) in MeCN (1 mL) and H_2O (1 mL). The mixture was stirred at 45 °C overnight and then was purified by reversed-phase preparative HPLC to give the title compound (60 mg, 69%). ^1H NMR (400 MHz, MeOH-d4) δ 7.71−7.64 (m, 2H), 7.52−7.44 (m, 1H), 7.44−7.33 (m, 2H), 7.18−7.10 (m, 1H), 6.55−6.47 (m, 2H), 4.15 (t, *J* = 8.0 Hz, 2H), 4.03 (s, 1H), 3.87−3.71 (m, 3H), 3.71−3.61 (m, 3H), 3.61−3.48 (m, 3H), 3.48−3.38 (m, 3H), 3.38−3.35 (m, 1H), 3.31−3.14 (m, 3H), 3.04 (t, *J* = 12.4 Hz, 1H), 2.98−2.79 (m, 2H), 2.58 (tt, *J* = 7.9, 4.8 Hz, 1H), 2.33−1.98 (m, 5H), 1.98−1.86 (m, 2H), 1.85−1.45 (m, 8H), 1.25 (s, 3H), 1.20−1.12 (m, 2H),

https://doi.org/10.1021/acs.jmedchem.1c00789
J. Med. Chem. 2021, 64, 10333−10349

Scheme 3. Synthesis of Compounds 19−26[a]

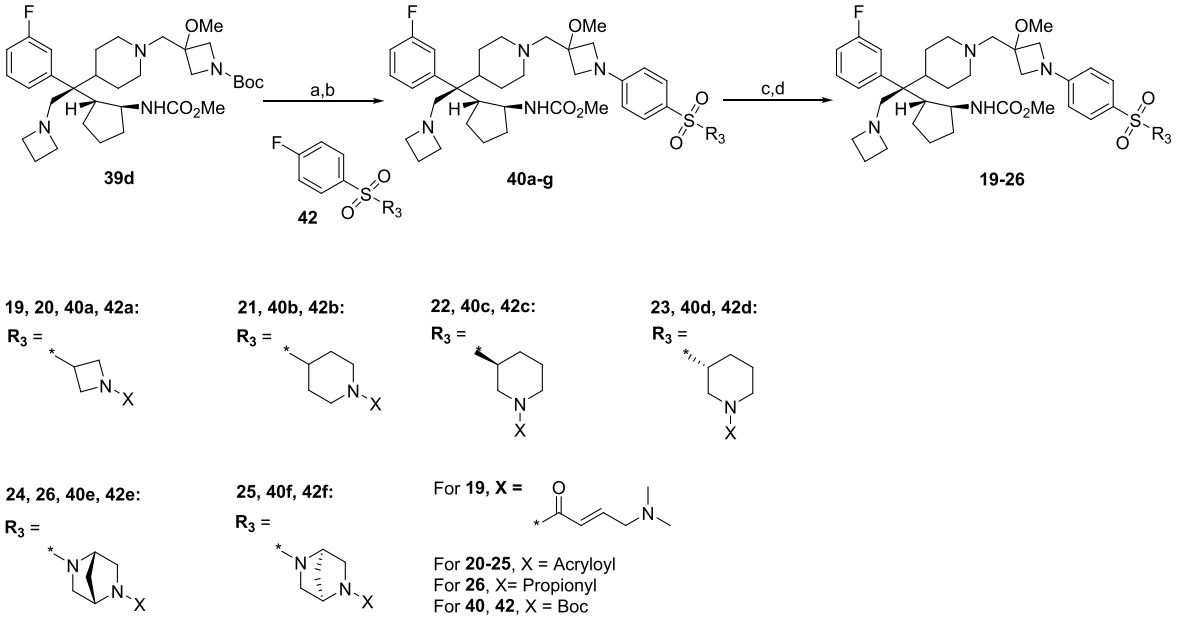

[a]Reagents and conditions: (a) TFA, DCM, rt; (b) **42**, K_2CO_3, DMSO, 80 °C; (c) TFA, DCM, rt; (d) (2*E*)-4-(dimethylamino)-2-butenoyl chloride hydrochloride, DIPEA, DCM, 0 °C to rt (**19**); acrylic anhydride, DIPEA, DCM, rt (**20−25**); propionic anhydride, DIPEA, DCM, rt (**26**).

1.05−0.96 (m, 2H); ESI-MS calcd for $C_{39}H_{56}FN_4O_5S$ $[M + H]^+$ = 711.40, found: 711.20.

*Methyl ((1S,2R)-2-((S)-2-(Azetidin-1-yl)-1-(1-((1-(4-(cyclopropylsulfonyl)phenyl)-3-fluoroazetidin-3-yl)methyl)-piperidin-4-yl)-1-(3-fluorophenyl)ethyl)cyclopentyl)carbamate (**14**).* Compound **14** was prepared from compounds **37**, **41a**, and **34** according to the procedure used to prepare compound **17**. ^{1}H NMR (400 MHz, MeOH-d4) δ 7.74−7.68 (m, 2H), 7.52−7.42 (m, 1H), 7.20−7.11 (m, 2H), 7.11−7.02 (m, 1H), 6.63−6.58 (m, 2H), 4.61−4.45 (m, 2H), 4.42−4.30 (m, 2H), 4.30−4.10 (m, 6H), 3.85−3.73 (m, 4H), 3.60 (t, J = 12.1 Hz, 2H), 3.55−3.42 (m, 1H), 3.16 (dt, J = 24.0, 12.4 Hz, 2H), 2.87−2.73 (m, 1H), 2.63−2.51 (m, 2H), 2.51−2.39 (m, 1H), 2.14−1.95 (m, 5H), 1.95−1.85 (m, 1H), 1.85−1.74 (m, 1H), 1.73−1.48 (m, 5H), 1.20−1.13 (m, 2H), 1.05−0.98 (m, 2H); ESI-MS calcd for $C_{36}H_{49}F_2N_4O_4S$ $[M + H]^+$ = 671.34, found: 671.26.

*Methyl ((1S,2R)-2-((S)-2-(Azetidin-1-yl)-1-(1-((1-(4-(cyclopropylsulfonyl)phenyl)-3-methylazetidin-3-yl)methyl)-piperidin-4-yl)-1-(3-fluorophenyl)ethyl)cyclopentyl)carbamate (**15**).* Compound **15** was prepared from compounds **37**, **41b**, and **34** according to the method used to produce compound **17**. ^{1}H NMR (400 MHz, MeOH-d4) δ 7.69−7.62 (m, 2H), 7.46 (td, J = 8.3, 6.3 Hz, 1H), 7.19−7.10 (m, 2H), 7.10−7.00 (m, 1H), 6.56−6.49 (m, 2H), 4.58−4.42 (m, 2H), 4.41−4.21 (m, 2H), 4.12 (d, J = 15.6 Hz, 1H), 3.92−3.71 (m, 6H), 3.59−3.42 (m, 3H), 3.38 (s, 3H), 3.18−2.98 (m, 2H), 2.87−2.72 (m, 1H), 2.56 (tt, J = 7.9, 4.8 Hz, 2H), 2.49−2.35 (m, 1H), 2.10−1.93 (m, 5H), 1.93−1.81 (m, 1H), 1.81−1.72 (m, 1H), 1.72−1.52 (m, 5H), 1.49 (s, 3H), 1.18−1.12 (m, 2H), 1.03−0.97 (m, 2H); ESI-MS calcd for $C_{37}H_{52}FN_4O_4S$ $[M + H]^+$ = 667.37, found: 667.27.

*Methyl ((1S,2R)-2-((S)-2-(Azetidin-1-yl)-1-(1-((1-(4-(cyclopropylsulfonyl)phenyl)-3-hydroxyazetidin-3-yl)methyl)-piperidin-4-yl)-1-(3-fluorophenyl)ethyl)cyclopentyl)carbamate (**16**).* Compound **16** was prepared from compounds **37**, **41c**, and **34** according to the procedure used to prepare compound **17**. ^{1}H NMR (400 MHz, MeOH-d4) δ 7.72−7.66 (m, 2H), 7.49 (td, J = 8.2, 6.2 Hz, 1H), 7.20−7.13 (m, 2H), 7.11−7.02 (m, 1H), 6.61−6.55 (m, 2H), 4.61−4.44 (m, 2H), 4.44−4.25 (m, 2H), 4.24−4.05 (m, 3H), 3.94 (d, J = 8.8 Hz, 2H), 3.80 (d, J = 15.6 Hz, 1H), 3.62 (t, J = 12.8 Hz, 2H), 3.49 (s, 3H), 3.22−3.02 (m, 2H), 2.90−2.75 (m, 1H), 2.58 (tt, J = 8.0, 4.8 Hz, 2H), 2.53−2.39 (m, 1H), 2.15−1.94 (m, 5H), 1.85 (d, J = 24.0 Hz, 3H), 1.69 (d, J = 12.5 Hz, 4H), 1.55 (d, J = 12.7 Hz, 1H), 1.22−1.12 (m, 2H), 1.06−0.97 (m, 2H); ESI-MS calcd for $C_{36}H_{50}FN_4O_5S$ $[M + H]^+$ = 669.35, found: 669.11.

*Methyl ((1S,2R)-2-((S)-2-(Azetidin-1-yl)-1-(1-((1-(4-(cyclopropylsulfonyl)phenyl)-3-methoxy-azetidin-3-yl)methyl)-piperidin-4-yl)-1-(3-fluorophenyl)ethyl)cyclopentyl)carbamate (**17**).* 10% Pd/C (344 mg, 10 wt %) was added to a solution of compound **37** (1.6 g, 3.24 mmol) in MeOH (50 mL) under a N_2 atmosphere. The solution was briefly vacuumed to remove the N_2 atmosphere and then put under a H_2 atmosphere; this was repeated three times. The mixture was then stirred for 2 h at rt under a H_2 atmosphere. The Pd/C catalyst was then filtered, and the solvent was removed by rotary evaporation to give compound **38**, which was not purified further. ^{1}H NMR (400 MHz, MeOH-d$_4$) δ 7.48−7.43 (m, 1H), 7.16−7.06 (m, 3H), 4.51−4.45 (m, 2H), 4.38−4.27 (m, 2H), 4.10 (d, J = 15.6 Hz, 1H), 3.77 (d, J = 15.2 Hz, 1H), 3.55−3.52 (m, 1H), 3.40−3.33 (m, 2H), 3.31 (s, 3H), 3.01−2.89 (m, 2H), 2.78−2.72 (m, 1H), 2.58−2.48 (m, 1H), 2.46−2.39 (m, 1H), 2.05−1.93 (m, 5H), 1.78−1.70 (m, 1H), 1.68−1.54 (m, 3H), 1.39−1.30 (m, 1H), 1.08−1.02 (m, 1H); ESI-MS calculated for $C_{23}H_{34}FN_3O_2$ $[M + H]^+$ = 404.26, found: 404.42.

Compound **38** (200 mg, 0.496 mmol), K_2CO_3 (206 mg, 1.49 mmol), and KI (8 mg, 0.0496 mmol) were added to a solution of compound **41d** (176 mg, 0.595 mmol) in MeCN (4 mL). The mixture was refluxed overnight. Then, the mixture was filtered through celite, concentrated, and purified with preparative HPLC to give **39d** (155 mg, 52%) as a white solid.

Compound **39d** (155 mg, 0.257 mmol) was dissolved in DCM (4 mL), and then TFA (380 μL, 5.14 mmol) was added. After stirring for 2 h at rt, the reaction mixture was then evaporated. The crude product was dissolved in DMSO (3 mL). Compound **34** (62 mg, 0.308 mmol) and K_2CO_3 (142 mg, 1.03 mmol) were added, and the mixture was stirred at 80 °C overnight. The mixture was quenched with H_2O and purified by reversed-phase preparative HPLC to give compound **17** (112 mg, 64%). ^{1}H NMR (400 MHz, MeOH-d4) δ 7.69−7.62 (m, 2H), 7.48−7.39 (m, 1H), 7.16−7.08 (m, 2H), 7.04 (d, J = 8.0 Hz, 1H), 6.59−6.53 (m, 2H), 4.57−4.39 (m, 2H), 4.38−4.20 (m, 4H), 4.11 (d, J = 15.6 Hz, 1H), 3.96−3.87 (m, 2H), 3.75 (d, J = 15.6 Hz, 1H), 3.61−3.50 (m, 4H), 3.50−3.39 (m, 5H), 3.15−2.97 (m, 2H), 2.84−2.70 (m, 1H), 2.59−2.46 (m, 2H), 2.46−2.33 (m, 1H), 2.10−1.90 (m, 5H), 1.90−1.71 (m, 3H), 1.71−1.57 (m, 4H), 1.56−1.44

https://doi.org/10.1021/acs.jmedchem.1c00789
J. Med. Chem. 2021, 64, 10333−10349

(m, 1H), 1.18−1.08 (m, 2H), 1.03−0.93 (m, 2H); ESI-MS calculated for $C_{37}H_{52}FN_4O_5S$ $[M + H]^+$ = 683.36, found: 683.16.

*Methyl 3-((4-((S)-2-(Azetidin-1-yl)-1-(3-fluorophenyl)-1-((1R,2S)-2-((methoxycarbonyl)amino)cyclopentyl)ethyl)piperidin-1-yl)-methyl)-1-(4-(cyclopropylsulfonyl)phenyl)azetidine-3-carboxylate (**18**).* Compound **18** was prepared from compounds **37**, **41e**, and **34** according to the procedure used to prepare compound **17**. ^{1}H NMR (400 MHz, MeOH-d_4) δ 7.73−7.67 (m, 2H), 7.52−7.41 (m, 1H), 7.20−7.10 (m, 2H), 7.06 (d, J = 7.9 Hz, 1H), 6.62−6.53 (m, 2H), 4.60−4.43 (m, 2H), 4.41−4.32 (m, 2H), 4.28 (dd, J = 8.3, 2.3 Hz, 2H), 4.13 (d, J = 15.6 Hz, 1H), 4.01 (dd, J = 8.4, 6.5 Hz, 2H), 3.88−3.79 (m, 4H), 3.79−3.72 (m, 3H), 3.69−3.60 (m, 2H), 3.55−3.40 (m, 1H), 3.25−3.08 (m, 2H), 2.83−2.72 (m, 1H), 2.58 (tt, J = 8.0, 4.8 Hz, 2H), 2.49−2.38 (m, 1H), 2.12−1.94 (m, 5H), 1.89 (s, 1H), 1.84−1.72 (m, 1H), 1.72−1.59 (m, 4H), 1.59−1.42 (m, 1H), 1.21−1.11 (m, 2H), 1.06−0.97 (m, 2H). ESI-MS calcd for $C_{38}H_{52}FN_4O_6S$ $[M + H]^+$ = 711.36, found: 711.15.

*Methyl ((1S,2R)-2-((S)-2-(Azetidin-1-yl)-1-(1-((1-(4-((1-((E)-4-(dimethylamino)but-2-enoyl)azetidin-3-yl)sulfonyl)phenyl)-3-methoxyazetidin-3-yl)methyl)piperidin-4-yl)-1-(3-fluorophenyl)ethyl)-cyclopentyl)carbamate (**19**).* Compound **19** was prepared from compounds **39d**, **42a**, and (2*E*)-4-(dimethylamino)-2-butenoyl chloride hydrochloride instead of acrylic anhydride according to the method used to produce compound **24**. ^{1}H NMR (400 MHz, MeOH-d_4) δ 7.70−7.64 (m, 2H), 7.44−7.36 (m, 1H), 7.12−7.04 (m, 2H), 7.00 (d, J = 8.0 Hz, 1H), 6.68 (dt, J = 15.3, 7.1 Hz, 1H), 6.58−6.52 (m, 2H), 6.41 (dt, J = 15.2, 1.3 Hz, 1H), 4.53−4.37 (m, 4H), 4.35−4.20 (m, 6H), 4.21−4.02 (m, 4H), 3.96−3.85 (m, 4H), 3.76−3.67 (m, 1H), 3.49 (s, 4H), 3.46−3.38 (m, 5H), 3.11−2.95 (m, 2H), 2.84 (s, 6H), 2.73 (d, J = 9.2 Hz, 1H), 2.48 (dt, J = 19.0, 9.5 Hz, 1H), 2.42−2.30 (m, 1H), 2.06−1.87 (m, 5H), 1.87−1.76 (m, 1H), 1.76−1.67 (m, 1H), 1.67−1.54 (m, 3H), 1.54−1.40 (m, 1H), 1.20−1.00 (m, 1H); ESI-MS calcd for $C_{43}H_{62}FN_6O_6S$ $[M + H]^+$ = 809.44, found: 809.28.

*Methyl ((1S,2R)-2-((S)-1-(1-((1-(4-((1-Acryloylazetidin-3-yl)-sulfonyl)phenyl)-3-methoxyazetidin-3-yl)methyl)piperidin-4-yl)-2-(azetidin-1-yl)-1-(3-fluorophenyl)ethyl)cyclopentyl)carbamate (**20**).* Compound **20** was prepared from compounds **39d** and **42a** according to the procedure used to produce compound **24**. ^{1}H NMR (400 MHz, MeOH-d4) δ 7.79−7.73 (m, 2H), 7.54−7.43 (m, 1H), 7.21−7.13 (m, 2H), 7.08 (d, J = 8.0 Hz, 1H), 6.32 (dd, J = 17.0, 9.5 Hz, 1H), 6.25 (dd, J = 17.0, 2.7 Hz, 1H), 5.77 (dd, J = 9.5, 2.7 Hz, 1H), 4.61−4.44 (m, 4H), 4.42−4.34 (m, 1H), 4.34−4.23 (m, 4H), 4.23−4.10 (m, 3H), 3.98 (dd, J = 9.7, 5.8 Hz, 2H), 3.79 (d, J = 15.6 Hz, 1H), 3.57 (s, 4H), 3.54−3.42 (m, 5H), 3.19−3.01 (m, 2H), 2.87−2.75 (m, 1H), 2.62−2.51 (m, 1H), 2.51−2.39 (m, 1H), 2.13−1.95 (m, 4H), 1.93−1.75 (m, 2H), 1.75−1.61 (m, 4H), 1.61−1.46 (m, 1H), 1.27−1.04 (m, 1H); ESI-MS calcd for $C_{40}H_{55}FN_5O_6S$ $[M + H]^+$ = 752.39, found: 752.21.

*Methyl ((1S,2R)-2-((S)-1-(1-((1-(4-((1-Acryloylpiperidin-4-yl)-sulfonyl)phenyl)-3-methoxyazetidin-3-yl)methyl)piperidin-4-yl)-2-(azetidin-1-yl)-1-(3-fluorophenyl)ethyl)cyclopentyl)carbamate (**21**).* Compound **21** was prepared from compounds **39d** and **42b** according to the procedure used to produce compound **24**. ^{1}H NMR (400 MHz, MeOH-d_4) δ 7.65−7.59 (m, 2H), 7.43 (td, J = 8.3, 6.2 Hz, 1H), 7.17−7.07 (m, 2H), 7.02 (d, J = 8.0 Hz, 1H), 6.69 (dd, J = 16.8, 10.7 Hz, 1H), 6.60−6.53 (m, 2H), 6.13 (dd, J = 16.8, 1.9 Hz, 1H), 5.69 (dd, J = 10.7, 1.9 Hz, 1H), 4.58 (d, J = 13.5 Hz, 1H), 4.47 (s, 2H), 4.38−4.22 (m, 5H), 4.22−4.04 (m, 2H), 3.92 (dd, J = 9.7, 5.9 Hz, 2H), 3.74 (d, J = 15.5 Hz, 1H), 3.60−3.49 (m, 4H), 3.45 (s, 5H), 3.37−3.31 (m, 1H), 3.16−2.95 (m, 3H), 2.83−2.72 (m, 1H), 2.72−2.61 (m, 1H), 2.57−2.46 (m, 1H), 2.45−2.29 (m, 1H), 2.11−1.89 (m, 6H), 1.88−1.79 (m, 1H), 1.78−1.70 (m, 1H), 1.70−1.54 (m, 4H), 1.54−1.35 (m, 3H), 1.13 (s, 1H); ESI-MS calcd for $C_{42}H_{59}FN_5O_6S$ $[M + H]^+$ = 780.42, found:780.33.

*Methyl ((1S,2R)-2-((S)-1-(1-((1-(4-(((S)-1-Acryloylpiperidin-3-yl)-sulfonyl)phenyl)-3-methoxyazetidin-3-yl)methyl)piperidin-4-yl)-2-(azetidin-1-yl)-1-(3-fluorophenyl)ethyl)cyclopentyl)carbamate (**22**).* Compound **22** was prepared from compounds **39d** and **42c** according to the procedure used to produce compound **24**. ^{1}H NMR (400 MHz, MeOH-d4) δ 7.73−7.67 (m, 2H), 7.53−7.43 (m, 1H), 7.21−7.13 (m, 2H), 7.08 (d, J = 8.0 Hz, 1H), 6.73 (dd, J = 16.8, 10.7 Hz, 1H), 6.66−6.59 (m, 2H), 6.16 (d, J = 16.8 Hz, 1H), 5.79−5.69 (m, 1H), 4.64 (d, J = 12.8 Hz, 1H), 4.53 (s, 2H), 4.44−4.22 (m, 5H), 4.16 (d, J = 15.6 Hz, 1H), 3.98 (dd, J = 9.6, 6.7 Hz, 3H), 3.80 (d, J = 15.6 Hz, 1H), 3.65−3.54 (m, 4H), 3.51 (s, 5H), 3.19−3.02 (m, 3H), 2.96 (t, J = 11.7 Hz, 1H), 2.91−2.76 (m, 1H), 2.64−2.50 (m, 1H), 2.50−2.38 (m, 1H), 2.22−2.10 (m, 1H), 2.10−1.96 (m, 5H), 1.96−1.85 (m, 2H), 1.85−1.75 (m, 2H), 1.75−1.59 (m, 4H), 1.59−1.42 (m, 2H), 1.17 (s, 1H); ESI-MS calcd for $C_{42}H_{59}FN_5O_6S$ $[M + H]^+$ = 780.42, found: 780.23.

*Methyl ((1S,2R)-2-((S)-1-(1-((1-(4-(((R)-1-Acryloylpiperidin-3-yl)-sulfonyl)phenyl)-3-methoxyazetidin-3-yl)methyl)piperidin-4-yl)-2-(azetidin-1-yl)-1-(3-fluorophenyl)ethyl)cyclopentyl)carbamate (**23**).* Compound **23** was prepared from compounds **39d** and **42d** according to the procedure used to produce compound **24**. ^{1}H NMR (400 MHz, MeOH-d4) δ 7.74−7.66 (m, 2H), 7.49 (td, J = 8.3, 6.4 Hz, 1H), 7.21−7.13 (m, 2H), 7.08 (d, J = 8.0 Hz, 1H), 6.73 (dd, J = 16.9, 10.8 Hz, 1H), 6.67−6.59 (m, 2H), 6.16 (d, J = 16.7 Hz, 1H), 5.79−5.70 (m, 1H), 4.64 (d, J = 12.8 Hz, 1H), 4.53 (s, 2H), 4.44−4.21 (m, 5H), 4.16 (d, J = 15.6 Hz, 1H), 3.98 (dd, J = 9.7, 6.6 Hz, 3H), 3.80 (d, J = 15.6 Hz, 1H), 3.57 (s, 4H), 3.52 (s, 5H), 3.19−3.02 (m, 3H), 2.96 (t, J = 11.6 Hz, 1H), 2.89−2.75 (m, 1H), 2.65−2.51 (m, 1H), 2.51−2.40 (m, 1H), 2.24−2.11 (m, 1H), 2.11−1.98 (m, 5H), 1.97−1.75 (m, 4H), 1.75−1.59 (m, 4H), 1.59−1.43 (m, 2H), 1.17 (s, 1H); ESI-MS calcd for $C_{42}H_{59}FN_5O_6S$ $[M + H]^+$ = 780.42, found: 780.19.

*Methyl ((1S,2R)-2-((S)-1-(1-((1-(4-(((1S,4S)-5-Acryloyl-2,5-diazabicyclo[2.2.1]heptan-2-yl)sulfonyl)phenyl)-3-methoxyazetidin-3-yl)methyl)piperidin-4-yl)-2-(azetidin-1-yl)-1-(3-fluorophenyl)-ethyl)cyclopentyl)carbamate (**24**).* Compound **39d** (2.20 g, 3.48 mmol) was dissolved in DCM (50 mL), and then trifluoroacetic acid (5.0 mL, 73.1 mmol) was added. After stirring for 2 h at rt, the reaction mixture was evaporated. The crude product was dissolved in DMSO (30 mL), and compound **42e** (1.49 g, 4.18 mmol) and K_2CO_3 (1.92 g, 13.9 mmol) were added. The mixture was stirred at 80 °C overnight. The mixture was quenched with H_2O and purified by reversed-phase preparative HPLC to give **40e** (1.66 g, 59%).

Compound **40e** (1.28 g, 1.50 mmol) was dissolved in DCM (25 mL), and then TFA (2.2 mL, 30.0 mmol) was added slowly. After stirring for 2 h at rt, the reaction mixture was evaporated to give the crude product without further purification. Acrylic anhydride (206 μL, 1.80 mmol) and Et_3N (623 μL, 4.50 mmol) were added to a solution of this crude product in DCM (20 mL). After stirring for 3 h at rt, the reaction mixture was evaporated and the residue was purified by reversed-phase preparative HPLC to give **24** (927 mg, 78%). ^{1}H NMR (400 MHz, MeOH-d4) δ 7.69−7.62 (m, 2H), 7.45 (q, J = 7.6 Hz, 1H), 7.18−7.08 (m, 2H), 7.07−6.98 (m, 1H), 6.66−6.59 (m, 0.5H), 6.59−6.52 (m, 2H), 6.32 (dd, J = 16.8, 10.0 Hz, 0.5H), 6.23 (ddd, J = 16.8, 2.1, 1.2 Hz, 1H), 5.72 (ddd, J = 10.0, 3.4, 2.1 Hz, 1H), 4.73 (s, 1H), 4.58−4.41 (m, 2H), 4.40−4.29 (m, 2H), 4.29−4.21 (m, 2H), 4.13 (d, J = 15.6 Hz, 1H), 3.91 (t, J = 8.7 Hz, 2H), 3.76 (d, J = 15.6 Hz, 1H), 3.63−3.54 (m, 2H), 3.54−3.50 (m, 3H), 3.50−3.45 (m, 4H), 3.44−3.38 (m, 1H), 3.34 (dd, J = 11.6, 2.2 Hz, 0.5H), 3.27 (s, 3H), 3.18 (dd, J = 9.6, 2.1 Hz, 0.5H), 3.14−2.97 (m, 2H), 2.85−2.71 (m, 1H), 2.61−2.47 (m, 1H), 2.47−2.34 (m, 1H), 2.13−1.90 (m, 4H), 1.89−1.72 (m, 4H), 1.72−1.57 (m, 4H), 1.49 (d, J = 12.8 Hz, 1H), 1.41−1.23 (m, 1H), 1.18−0.98 (m, 1H); ^{13}C NMR (101 MHz, MeOH-d4) δ 165.14, 162.70, 159.82, 154.38 (d, J = 4.4 Hz), 131.20 (d, J = 8.4 Hz), 130.26 (d, J = 6.2 Hz), 129.25, 129.10, 129.05, 128.76, 126.37 (d, J = 3.9 Hz), 125.56, 117.05 (d, J = 23.1 Hz), 115.61 (d, J = 21.2 Hz), 112.28, 74.16, 61.38, 60.53, 59.72, 58.61 (d, J = 6.7 Hz), 57.53, 56.72, 55.74, 55.06, 54.84, 52.96, 51.73, 50.94, 41.32, 37.54, 35.90, 33.72, 26.90, 26.20, 25.77, 21.21, 17.08; ESI-MS calcd for $C_{42}H_{58}FN_6O_6S$ $[M + H]^+$ = 793.41, found: 793.16.

*Methyl ((1S,2R)-2-((S)-1-(1-((1-(4-(((1R,4R)-5-Acryloyl-2,5-diazabicyclo[2.2.1]heptan-2-yl)sulfonyl)phenyl)-3-methoxyazetidin-3-yl)methyl)piperidin-4-yl)-2-(azetidin-1-yl)-1-(3-fluorophenyl)-ethyl)cyclopentyl)carbamate (**25**).* Compound **25** was prepared from compounds **39d** and **42f** according to the procedure used to produce compound **24**. ^{1}H NMR (400 MHz, MeOH-d4) δ 7.72−7.67 (m, 2H), 7.49 (q, J = 7.7 Hz, 1H), 7.21−7.12 (m, 2H), 7.07 (d, J = 8.0

https://doi.org/10.1021/acs.jmedchem.1c00789
J. Med. Chem. 2021, 64, 10333−10349

Hz, 1H), 6.69−6.62 (m, 0.5H), 6.62−6.57 (m, 2H), 6.36 (dd, *J* = 16.8, 10.0 Hz, 0.5H), 6.30−6.23 (m, 1H), 5.75 (ddd, *J* = 10.0, 3.8, 2.1 Hz, 1H), 4.77 (s, 1H), 4.53 (s, 2H), 4.36 (s, 2H), 4.32−4.24 (m, 2H), 4.16 (d, *J* = 15.7 Hz, 1H), 3.95 (dd, *J* = 9.5, 4.8 Hz, 2H), 3.84−3.75 (m, 1H), 3.67−3.57 (m, 2H), 3.57−3.54 (m, 3H), 3.54−3.49 (m, 4H), 3.48−3.42 (m, 1H), 3.38 (dd, *J* = 11.7, 2.1 Hz, 0.5H), 3.31−3.27 (m, 3H), 3.22 (dd, *J* = 9.5, 2.1 Hz, 0.5H), 3.18−3.00 (m, 2H), 2.81 (d, *J* = 9.5 Hz, 1H), 2.62−2.38 (m, 2H), 2.13−1.95 (m, 4H), 1.93−1.76 (m, 3H), 1.76−1.61 (m, 4H), 1.54 (d, *J* = 12.8 Hz, 1H), 1.46−1.35 (m, 1H), 1.35−1.27 (m, 1H), 1.15 (s, 1H); ESI-MS calcd for $C_{42}H_{58}FN_6O_6S$ $[M + H]^+$ = 793.41, found: 793.12.

*Methyl ((1S,2R)-2-((S)-2-(Azetidin-1-yl)-1-(3-fluorophenyl)-1-(1-((3-methoxy-1-(4-(((1S,4S)-5-propionyl-2,5-diazabicyclo[2.2.1]-heptan-2-yl)sulfonyl)phenyl)azetidin-3-yl)methyl)piperidin-4-yl)-ethyl)cyclopentyl)carbamate (**26**).* Compound **26** was prepared from compounds **39d**, **42e**, and propionic anhydride instead of acrylic anhydride according to the procedure used to produce compound **24**. ^{1}H NMR (400 MHz, MeOH-d4) δ 7.72−7.66 (m, 2H), 7.53−7.44 (m, 1H), 7.20−7.12 (m, 2H), 7.08 (d, *J* = 8.0 Hz, 1H), 6.64−6.55 (m, 2H), 4.74−4.43 (m, 4H), 4.43−4.31 (m, 2H), 4.31−4.24 (m, 2H), 4.21−4.10 (m, 1H), 3.96 (t, *J* = 8.5 Hz, 2H), 3.84−3.75 (m, 1H), 3.56 (s, 3H), 3.54−3.44 (m, 6H), 3.42−3.35 (m, 0.5H), 3.30−3.25 (m, 2H), 3.19 (dd, *J* = 9.5, 2.0 Hz, 0.5H), 3.17−3.02 (m, 2H), 2.81 (d, *J* = 9.4 Hz, 1H), 2.61−2.49 (m, 1H), 2.50−2.40 (m, 1H), 2.40−2.29 (m, 1H), 2.22−2.08 (m, 2H), 2.08−1.95 (m, 5H), 1.94−1.84 (m, 1H), 1.84−1.73 (m, 2H), 1.73−1.59 (m, 4H), 1.59−1.48 (m, 1H), 1.37−1.26 (m, 1H), 1.11 (t, *J* = 7.5 Hz, 2H), 1.05 (t, *J* = 7.5 Hz, 2H); ESI-MS calcd for $C_{42}H_{60}FN_6O_6S$ $[M + H]^+$ = 795.43, found: 827.32.

*Methyl ((1S,2R)-2-((S)-(1-Benzylpiperidin-4-yl)(cyano)(3-fluorophenyl)methyl)cyclopentyl)-carbamate (**28**).* Compound **27** (2.28 g, 4.64 mmol) was dissolved in dichloromethane (14 mL), and TFA (6.9 mL, 92.9 mmol) was added slowly. After stirring for 2 h at rt, the reaction mixture was concentrated under vacuum. The crude product was dissolved in dry dichloromethane (50 mL). Then, Et_3N (5.2 mL, 37.1 mmol) and dimethyl dicarbonate (1.24 mg, 9.28 mmol) were added at 0 °C. After stirring for 2 h at rt, the reaction mixture was concentrated under vacuum. The residue was purified by column chromatography (silica gel, DCM/MeOH 20:1 to 10:1) to give **28** (1.86 g, 89%). ^{1}H NMR (400 MHz, MeOH-d4) δ 7.43 (td, *J* = 8.0, 6.0 Hz, 1H), 7.38−7.23 (m, 7H), 7.11 (tdd, *J* = 8.3, 2.5, 1.0 Hz, 1H), 3.88 (q, *J* = 7.0 Hz, 1H), 3.49 (s, 2H), 3.46 (s, 3H), 2.99−2.89 (m, 2H), 2.84 (td, *J* = 8.3, 6.9 Hz, 1H), 2.15−2.04 (m, 2H), 2.04−1.94 (m, 3H), 1.88−1.76 (m, 1H), 1.72−1.60 (m, 3H), 1.60−1.48 (m, 2H), 1.43−1.34 (m, 1H), 1.26 (td, *J* = 12.7, 4.0 Hz, 1H); ESI-MS calcd for $C_{27}H_{33}FN_3O_2$ $[M + H]^+$ = 450.26, found: 450.08.

*Methyl ((1S,2R)-2-((S)-2-Amino-1-(1-benzylpiperidin-4-yl)-1-(3-fluorophenyl)ethyl)cyclopentyl)carbamate (**29**).* Compound **28** (7.62 g, 16.9 mmol) was added to a dry RB-flask, which was then covered with a Kimwipe and put in a desiccator that was put under vacuum for 1−2 days. After the vacuuming step, the flask was removed from the desiccator and quickly capped with a septum and the system was vacuumed under a N_2 atmosphere. Anhydrous toluene (150 mL) was added to the flask and then was cooled to 0 °C in an ice-bath. Diisobutylaluminum hydride (25% in toluene, 45.2 mL, 67.8 mmol) was injected into the reaction mixture slowly at 0 °C with a syringe under stirring. After 4 h, the reaction was quenched with potassium sodium tartrate (aq). The mixture was stirred vigorously overnight and was extracted with EtOAc three times. The organic solvent was washed with brine, dried with Na_2SO_4, filtered, and concentrated under rotatory vacuum. The residue was redissolved in MeOH (200 mL), $NaBH_4$ (2.56 g, 67.8 mmol) was added slowly at 0 °C, and the reaction mixture was stirred at rt overnight. The reaction mixture was concentrated and diluted with water and extracted with DCM three times. The organic solvent was washed with brine, dried with Na_2SO_4, filtered, and concentrated under rotatory vacuum to give crude product **29** (6.52 g, 85%), which was used without further purification. ^{1}H NMR (400 MHz, MeOH-d_4) δ 7.37−7.24 (m, 6H), 7.08−7.00 (m, 2H), 6.99−6.92 (m, 1H), 3.64−3.51 (m, 2H), 3.39−3.25 (m, 2H), 3.23 (s, 3H), 3.08 (s, 2H), 2.93−2.81 (m, 1H), 2.81−2.72 (m, 1H), 2.60 (q, *J* = 9.4 Hz, 1H), 2.00−1.92 (m, 1H), 1.90 (s, 2H), 1.89−1.68 (m, 4H), 1.64−1.52 (m, 2H), 1.52−1.41 (m, 2H), 1.40−1.30 (m, 1H); ESI-MS calcd for $C_{27}H_{37}FN_3O_2$ $[M + H]^+$ = 454.29, found: 454.24.

*Methyl ((1S,2R)-2-((S)-1-(1-Benzylpiperidin-4-yl)-2-((tert-butoxycarbonyl)amino)-1-(3-fluorophenyl)ethyl)cyclopentyl)-carbamate (**30**).* Compound **29** (2.68 g, 5.91 mmol) was dissolved in dry dichloromethane (50 mL). Then, Et_3N (1.2 mL, 8.87 mmol) and di-*tert*-butyl dicarbonate (2.71 mL, 11.8 mmol) were added. After stirring for 2 h at rt, the reaction mixture was concentrated under vacuum. The residue was purified by column chromatography (silica gel, DCM/MeOH 20:1 to 8:1) to give **30** (2.30 g, 70%). ^{1}H NMR (400 MHz, MeOH-d4) δ 7.42−7.18 (m, 8H), 6.99 (td, *J* = 8.1, 2.3 Hz, 1H), 4.10 (q, *J* = 6.8 Hz, 1H), 3.84−3.73 (m, 1H), 3.70−3.60 (m, 1H), 3.54 (s, 3H), 3.49 (s, 2H), 3.00−2.85 (m, 2H), 2.45 (q, *J* = 8.4 Hz, 1H), 2.05−1.92 (m, 3H), 1.92−1.78 (m, 2H), 1.67−1.51 (m, 4H), 1.47 (s, 9H), 1.42−1.30 (m, 3H), 1.25−1.15 (m, 1H); ESI-MS calcd for $C_{32}H_{45}FN_3O_4$ $[M + H]^+$ = 554.34, found: 554.09.

*Methyl ((1S,2R)-2-((S)-2-((tert-Butoxycarbonyl)amino)-1-(1-((1-(4-(cyclopropylsulfonyl)phenyl)azetidin-3-yl)methyl)piperidin-4-yl)-1-(3-fluorophenyl)ethyl)cyclopentyl)carbamate (**31**).* Palladium on carbon (150 mg, 10 wt %) was added to a solution of compound **30** (500 mg, 0.903 mmol) in MeOH (10 mL) under a N_2 atmosphere. The solution was briefly vacuumed to remove the N_2 atmosphere and then put under a H_2 atmosphere; this was repeated three times. The mixture was then stirred for 6 h at rt under a H_2 atmosphere. The Pd/C catalyst was then filtered, and the solvent was removed by rotary evaporation. The residue was then redissolved in acetonitrile (5 mL). K_2CO_3 (374 mg, 2.71 mmol), KI (15 mg, 0.0903 mmol), and **36** (374 mg, 1.08 mmol) were added to the solution. The mixture was stirred at 80 °C overnight. Then, the mixture was concentrated in vacuum and purified by reversed-phase preparative HPLC to give **31** (399 mg, 62%). ESI-MS calcd for $C_{38}H_{54}FN_4O_6S$ $[M + H]^+$ = 713.37, found: 713.15.

*Cyclopropyl(4-fluorophenyl)sulfane (**33**).* To a stirred solution of **32** (2.0 mL, 18.7 mmol) in DMSO (50 mL) under a N_2 atmosphere were added cyclopropyl bromide (1.6 mL, 20.6 mmol) and *t*-BuONa (4.49 g, 46.8 mmol). Then the reaction mixture was heated at 80 ° C for 24 h. After cooling to rt, the mixture was poured into H_2O (250 mL) and extracted with Et_2O three times. The combined organic phases were washed with brine, dried over Na_2SO_4, and concentrated in vacuum. The residue was purified by column chromatography (silica gel, hexane/EtOAc 100:1 to 15:1) to give **33** (1.32 g, 42%). Spectral data was identical to the literature compound.[30]

*1-(Cyclopropylsulfonyl)-4-fluorobenzene (**34**).* *m*-CPBA (4.28 g, 17.4 mmol, 70%) was added to a stirred solution of **33** (1.46 g, 8.68 mmol) in DCM (80 mL) at 0 °C. After 2 h, the reaction mixture was quenched with 1 M NaOH (aq.) and extracted with DCM three times. The combined organic phases were washed with brine, dried over Na_2SO_4, and concentrated in vacuum. The residue was purified by column chromatography (silica gel, hexane/EtOAc 10:1 to 1:1) to give **34** (1.58 g, 91%). ^{1}H NMR (400 MHz, $CDCl_3$) δ 7.97−7.91 (m, 2H), 7.28−7.22 (m, 2H), 2.47 (tt, *J* = 8.0, 4.8 Hz, 1H), 1.40−1.34 (m, 2H), 1.11−1.03 (m, 2H).

*Methyl 1-(4-(Cyclopropylsulfonyl)phenyl)azetidine-3-carboxylate (**35**).* Compound **34** (819 mg, 4.09 mmol) was dissolved in DMSO (20 mL), methyl azetidine-3-carboxylate hydrochloride (620 mg, 4.09 mmol), and K_2CO_3 (2.26 g, 16.4 mmol) were added. The mixture was quenched with water and extracted with EA three times. The combined organic phases were washed with brine, dried over Na_2SO_4, and concentrated in vacuum. The residue was purified by column chromatography (silica gel, hexane/EtOAc 2:1 to 1:2) to give **35** (729 mg, 60%). ^{1}H NMR (400 MHz, $CDCl_3$) δ 7.71−7.66 (m, 2H), 6.46−6.41 (m, 2H), 4.21−4.10 (m, 4H), 3.76 (s, 3H), 3.60 (tt, *J* = 8.6, 6.0 Hz, 1H), 2.40 (tt, *J* = 8.0, 4.8 Hz, 1H), 1.32−1.22 (m, 2H), 1.01−0.90 (m, 2H); ESI-MS calcd for $C_{14}H_{18}NO_4S$ $[M + H]^+$ = 296.10, found: 259.82.

*(1-(4-(Cyclopropylsulfonyl)phenyl)azetidin-3-yl)methyl Methanesulfonate (**36**).* Compound **35** (729 mg, 2.47 mmol) was dissolved in THF (30 mL), and $LiAlH_4$ (4.9 mL, 1 M in THF) was added at 0

https://doi.org/10.1021/acs.jmedchem.1c00789
J. Med. Chem. 2021, 64, 10333−10349

°C. After 4 h, the reaction was quenched with potassium sodium tartrate (aq). The mixture was stirred vigorously overnight and was extracted with EtOAc three times. The organic solvent was washed with brine, dried with Na_2SO_4, filtered, and concentrated under rotatory vacuum. The residue was redissolved in DCM (25 mL), and Et_3N (1.0 mL, 7.41 mmol) and methanesulfonyl chloride (230 μL, 2.96 mmol) were added. After stirring under rt for 1 h, the reaction was quenched with water and extracted with DCM three times. The combined organic phases were washed with brine, dried over Na_2SO_4, and concentrated in vacuum. The residue was purified by column chromatography (silica gel, DCM/MeOH 20:1 to 15:1) to give **36** (699 mg, 82%). ^{1}H NMR (400 MHz, $CDCl_3$) δ 7.73−7.67 (m, 2H), 6.46−6.40 (m, 2H), 4.46 (d, *J* = 6.7 Hz, 2H), 4.10 (t, *J* = 8.1 Hz, 2H), 3.81 (dd, *J* = 8.0, 5.0 Hz, 2H), 3.25−3.13 (m, 1H), 3.06 (s, 3H), 2.41 (tt, *J* = 8.0, 4.8 Hz, 1H), 1.32−1.25 (m, 2H), 1.00−0.93 (m, 2H); ESI-MS calcd for $C_{14}H_{20}NO_5S_2$ $[M + H]^+$ = 346.08, found: 345.92.

*tert-Butyl (1S,4S)-5-((4-Fluorophenyl)sulfonyl)-2,5-diazabicyclo-[2.2.1]heptane-2-carboxylate (**42e**).* (1*S*,4*S*)-2-Boc-2,5-diazabicyclo-[2.2.1]heptane (1.0 g, 5.05 mmol) was added to a solution of 4-fluorobenzenesulfonyl chloride (1.08 g, 5.55 mmol) and Et_3N (2.1 mL, 15.2 mmol) in 40 mL of DCM. After 5 h, H_2O was added and the reaction was extracted three times with DCM, concentrated, and purified by column chromatography (silica gel, hexane/EtOAc 3:1 to 1:2) to give **42e** as a white solid. ^{1}H NMR (400 MHz, $CDCl_3$) δ 7.93−7.80 (m, 2H), 7.21 (td, *J* = 8.7, 2.3 Hz, 2H), 4.50−4.30 (m, 2H), 3.40 (ddd, *J* = 23.1, 14.1, 9.2 Hz, 2H), 3.29−3.13 (m, 2H), 1.71 (dd, *J* = 15.1, 10.1 Hz, 1H), 1.41 (d, *J* = 12.2 Hz, 9H), 1.33 (t, *J* = 8.0 Hz, 1H). ESI-MS calcd for $C_{16}H_{22}FN_2O_4S$ $[M + H]^+$ = 357.13, found: 357.01.

Fluorescence Polarization (FP)-Based Binding Assay. Compound binding was measured using an FP assay as described previously.[27] Briefly, 5 μL of compounds at various concentrations in dimethyl sulfoxide (DMSO) solution was added to 195 μL of a mixture of menin and the fluorescein-labeled tracer (compound **37** in our previous publication[27]) in the assay buffer (phosphate-buffered saline, 100 μg/mL bovine γ-globulin, with 0.01% Triton X-100), and the mixture was incubated for 1 h at rt. Final concentrations of the menin protein and the fluorescein-labeled tracer were 4 and 2 nM, respectively. FP values were measured using an Infinite M-1000 plate reader (Tecan, Morrisville, NC). The IC_{50} values were determined by nonlinear regression fitting of the sigmoidal dose-dependent FP decreases as a function of total compound concentrations using the GraphPad Prism 5.0 software.

Cell Growth Evaluation. MLLr and MLL wild-type leukemia cell lines were plated in 96-well tissue culture plates in triplicate. Compounds were added in a 9-point dose response curve starting from 10 μM top concentration with 1:3 serial dilutions. Compounds were diluted in DMSO to a final concentration of 0.1% DMSO in media. One column on each plate was designated for the 0.1% DMSO vehicle control. Total cellular ATP levels were measured using the CellTiter-Glo (Promega) reagent on the day of cell plating (day 0 readout). The cells were then incubated at 37 °C in RPMI 1640 media (Gibco) and 5% CO_2 for 4 days, and total cellular ATP levels were measured again using the CellTiter-Glo reagent. ATP standard curves were generated on both day 0 and day 4. IC_{50} was calculated using the GraphPad Prism data analysis software. The catalog numbers for each cell lines are MV4;11 (CRL-9591, ATCC), OCI-AML4 (ACC-729, DSMZ), MOLM-13 (C0003003, AddexBio), SEM (ACC-546, DSMZ), KOPN8 (ACC-552, DSMZ), RS4;11(CRL-1873, ATCC), HL-60 (CCL-240, ATCC), K562 (CCL-243, ATCC), and MEG-1 (CRL-2021, ATCC).

Computational Modeling. This modeling is based on the crystal structure of Menin bound to inhibitor M-808 (PDB id: 6WNH), which was obtained from the RCSB. All of the modeling was conducted using the software package MOE.[38] The 6WNH structure was imported into MOE and prepared for modeling in a standard fashion. Briefly, the crystallization additives were removed, and crystallographic water molecules were retained. There were three chain breaks due to unresolved residues. Ends for two of the breaks were capped. The third break only involved three missing residues, which were built in using MOE utilities. All three of the breaks were distant from the binding site. Both the N- and C-termini were capped due to unresolved residues. Missing sidechains were built in using MOE utilities. Both termini and the missing sidechains were distant from the binding site except for the sidechain of Arg332, which was approximately 5 Å from the tail of the inhibitor. The system was parameterized with AMBER 10. The Cys329 sulfur atom was displayed as being covalently bound to the inhibitor. That bond was removed, and the cysteine residue was allowed to move away from the inhibitor using energy minimization keeping all other atoms fixed. Bond orders for the inhibitor were checked, the inhibitor was protonated appropriately, and then partial charges for it were obtained using the MMFF94 (modified) force field since the inhibitor exceeds the AM1-BCC size limits in MOE. All heavy atoms were fixed, and the positions of the hydrogen atoms were allowed to relax using energy minimization. This prepared structure was used as the starting point for the modeling of the inhibitors. Compounds **24** and **25** were each separately built into the Menin binding site by modifying the M-808 inhibitor. Once the new inhibitor had been built into the binding site, the whole system was assigned AMBER 10 parameters. Following that, the inhibitor was assigned partial charges using AM1-BCC. (Because of the smaller sizes of compounds **24** and **25**, it was possible to use AM1-BCC.) A series of minimizations were then conducted to generate the final models for the **24** and **25** inhibitors in complex with Menin. The positions of the hydrogen atoms were first relaxed with energy minimization while all heavy atoms were held fixed. Next, portions of the inhibitor that had been modified to create inhibitors **24** and **25** were relaxed using energy minimization. Sidechains of any residue having at least one atom within 6 Å of the inhibitor were then also allowed to relax. Finally, all of the atoms of the inhibitor and any residue with at least one atom within 6 Å of the inhibitor were allowed to relax with energy minimization.

Crystallization and Structure Determination. Menin (residues 2−610 containing a deletion from 460 to 519) was purified as previously described.[26] For crystallization, Menin (25 mg/mL in 25 mM Tris 8.0, 150 mM NaCl, and 5 mM DTT) was mixed with M-1121 in a protein to compound ratio of 1:1.2 and then immediately set up for crystallization at 4 °C. All crystals grew in drops containing 1 μL of the complex and 1 μL of well solution (1.96 M NaCl, 89 mM Bis-Tris pH 6.8, 0.178 M $MgCl_2$, and 10.7 mM Pr Acetate). Crystals were cryoprotected by progressively soaking crystals in well solution with increasingly higher amounts of sodium formate (1−5 M in 1 M steps). Diffraction data were collected on an Eiger 9 M detector at the Advanced Photon Source LS-CAT 21-ID-D beamline at the Argonne National Laboratory. All data were processed with HKL2000.[33] The structure of menin-1121 was solved by molecular replacement (Molrep[34]) using the protein structure from PDB ID 6WNH as the search model. The structure went through iterative rounds of electron density fitting and structural refinement using Coot[35] and Buster,[36] respectively. The coordinates and restraint files for the ligands were created from smiles in Grade[37] with the mogul+qm option. The initial Fo-Fc electron density map showed the presence of one compound covalently bound to C329 (Figure S1). The following regions were disordered in the structure: 71−73, 386−401, 528−547, and 582−610. Data collection and structural refinement statistics are shown in Table S1.

Mass Spectroscopic Analysis of the Human Menin Protein Incubated with Menin Inhibitors. Samples of menin (25 mg/mL in 25 mM Tris 8.0, 150 mM NaCl, and 5 mM DTT) were incubated with compounds in a protein-to-compound molar ratio of 1:1.2 for 1 h or overnight at 4 °C. Following incubation, the sample was diluted to 1 mg/mL with H_2O. Each sample (0.1 mL) was subjected to a reversed-phase HPLC column (Phenomenex Aeris widepore C4 column 3.6 μM, 50 mm × 2.10 mm) at a flow rate of 0.5 mL/min in H_2O with 0.2% (v/v) HCOOH. The protein was eluted using a gradient of 5−100% MeCN with 0.2% (v/v) HCOOH over 4 min. The liquid chromatography−mass spectrometry (LC−MS) experiment (Agilent Q-TOF 6545) was carried out under the following conditions: fragmentor voltage, 300 V; skimmer voltage, 75 V; nozzle voltage, 100 V; sheath gas temperature, 350 °C; and drying gas

https://doi.org/10.1021/acs.jmedchem.1c00789
J. Med. Chem. 2021, 64, 10333−10349

temperature, 325 °C. The MassHunter Qualitative Analysis software (Agilent) was used to analyze the data. Intact protein masses were obtained using the maximum entropy deconvolution algorithm.

Real-Time PCR. Total RNA was isolated from either cell grown *in vitro* or bone marrow samples enriched for human CD45$^+$ cells by an EasySep Human CD45 Depletion Kit (STEMCELL Technologies) using an RNeasy kit (QIAGEN) according to the manufacturer's protocol. The cDNA was generated using a High-Capacity cDNA Reverse Transcription Kit (Applied Biosystems). Real-time PCR amplifications of HOXA9, MEIS1, ITGAM, GAPDH, and HPRT1genes were carried out with primers specific for each gene, using TaqMan gene expression assays (Applied Biosystems). Relative quantification of each gene transcript was calculated by a comparative cycle threshold (Ct) method. The results were presented as relative expression to vehicle treatment after normalizing to an internal loading control GAPDH or HPRT1. The catalog numbers for primers of each genes are HOXA9 (Hs00365956_m1), MEIS1 (Hs00180020_m1), ITGAM (Hs00167304_m1), GAPDH (Hs99999905_m1), and HPRT1 (Hs99999909_m1).

Plasma Protein Binding. To determine plasma protein binding using a dialysis method, dialysis buffer was loaded into the receiver side of a dialysis chamber and plasma or dialysis buffer spiked with M-1121 (1 μM), or plasma spiked with warfarin (1 μM) or quinidine (1 μM) was loaded into the donor side of the dialysis chambers and the dialysis block was shaken at 37 °C for 5 h. After incubation, samples from both the donor and receiver sides of the dialysis apparatus were added to a 96-well plate and mixed with the same volume of opposite matrices (blank buffer to plasma and blank plasma to buffer). To prepare 0 h samples, plasma or dialysis buffer spiked with M-1121 (1 μM) or 100 μL of plasma spiked with warfarin (1 μM) or quinidine (1 μM) was added to a 96-well plate and mixed with the same volume of blank buffer. Zero-hour samples were stored at −20 °C until analysis. At the time of analysis, all samples were quenched with acetonitrile containing the internal standard imipramine. After quenching, assay plates were shaken followed by centrifugation. Supernatants were removed and added to a new 96-well plate and then diluted with Mill-Q water before being analyzed by liquid chromatography with tandem mass spectrometry. The peak area ratio between the sample and the internal standard was used to calculate percent bound, percent unbound, and recovery.

Flow Cytometry. Bone marrow cells were collected, and cell suspensions were filtered through a 70 μM cell strainer and washed with PBS. Red blood cells were removed by using 1× RBC lysis buffer (Sigma, cat#R7757.) Samples were washed twice with pre-cold PBS and stained with a fixable viability stain (BD, cat# 565388) followed by human FcR blocker treatment (BD, cat#564219). Next, cells were stained with an Anti-human CD45 (BD, cat#563204), Anti-human CD33 (BD, cat#555626), and Anti-human CD11b (BD, cat#562721) antibody mixture at 4 °C for 40 min in the dark. Samples were suspended with cell staining buffer and analyzed on a Thermo Attune NxT flow cytometer.

Animal Experiments. Animal experiments were performed under the guidelines of the University of Michigan Committee for Use and Care of Animals and using an approved animal protocol (PI, Shaomeng Wang) or in accordance with ChemPartner approved Institutional Animal Care and Use Committee (IACUC) protocols.

***In Vivo* Efficacy Studies in an MV4;11 Human AML Xenograft Model in Mice.** Five−six-week-old female C.B.-17 SCID mice were purchased from Charles River and implanted subcutaneously in the right flank with MV4;11 cells at an inoculum of 5 × 10^6 cells/mouse (cell suspension and Matrigel at a 1:1 ratio.) Once tumors reached 200 mm^3, mice were randomized into vehicle (0.5% MC (400 cP) + 0.2% tween 80 (w/w)) or M-1121-treated groups. Treatment was administered daily by oral gavage (QD) at 10 mL/kg.

Body weights were measured daily, and tumor volume was measured three times a week using Vernier calipers. Tumor volume was calculated using the formula 0.5 × W × W × L, with W being the tumor width and L being the tumor length. Results were graphed as mean ± standard error (SEM). Graphing and statistical analysis were performed using GraphPad Prism 8.00 (GraphPad Software).

***In Vivo* Studies in a Luciferase-Tagged MV4;11 AML Xenograft Model.** Five−six-week-old female NCG mice obtained from Charles River Laboratories were implanted systemically via tail vein injection with Luciferase-tagged-MV;411 cells at an inoculum level of 5 × 10^6 cells/mouse in serum free media. The severity of the disease was monitored by an IVIS SpectrumCT Imaging System twice weekly as recommended by the manufacturer (PerkinElmer) until disease burden reached the log phase (27 days post implant.) Mice were randomized into two groups, vehicle and M-1121, that were formulated and administered as mentioned above. Mice were treated for 4 days, and bone marrow samples were collected 48 h after the last dose and subjected to either staining for flow cytometry evaluation or human CD45$^+$ cell enrichment for downstream gene expression evaluation by RT-qPCR.

Bioluminescence Imaging. Mice implanted with Luciferase-tagged MV4;11 cells were peritoneally injected with luciferin potassium salt (PerkinElmer, cat#122799-5) at a dose of 150 mg/kg before undergoing anesthesia with 3% isoflurane (Patterson Veterinary Supply, cat#07-806-3204) in air in an anesthesia induction chamber. Bioluminescence imaging was performed using an IVIS imaging system, and mice were imaged approximately 5 min after substrate injection. Acquisition settings (binning and duration) were set up depending upon tumor activity at the time of acquisition.

■ ASSOCIATED CONTENT

Supporting Information

The Supporting Information is available free of charge at https://pubs.acs.org/doi/10.1021/acs.jmedchem.1c00789.

Crystallography data collection and refinement statistics. *In vivo* pharmacokinetics and efficacy data of compounds **10**, **17**, **24** (M-1121) in mice. Purity and spectral data of M-1121. Method for computational modeling for compounds **24** and **25** (PDF)

A molecular string file for all the final target compounds (CSV)

Modeled structures of compounds **24** and **25** in complex with the menin protein (PBD) (PBD)

Accession Codes

The coordinates for M-1121 complexed with menin have been deposited into the Protein Data Bank with the PDB code 7M4T. Authors will release the atomic coordinates upon publication of this article.

■ AUTHOR INFORMATION

Corresponding Author

Shaomeng Wang − *Rogel Cancer Center, Department of Internal Medicine, Department of Pharmacology, and Department of Medicinal Chemistry, Medical School, University of Michigan, Ann Arbor, Michigan 48109, United States;* orcid.org/0000-0002-8782-6950; Email: shaomeng@umich.edu

Authors

Meng Zhang − *Rogel Cancer Center and Department of Internal Medicine, University of Michigan, Ann Arbor, Michigan 48109, United States*

Angelo Aguilar − *Rogel Cancer Center and Department of Internal Medicine, University of Michigan, Ann Arbor, Michigan 48109, United States*

Shilin Xu − *Rogel Cancer Center and Department of Internal Medicine, University of Michigan, Ann Arbor, Michigan 48109, United States;* orcid.org/0000-0003-0845-0260

Liyue Huang − *Rogel Cancer Center and Department of Internal Medicine, University of Michigan, Ann Arbor, Michigan 48109, United States*
Krishnapriya Chinnaswamy − *Life Sciences Institute, University of Michigan, Ann Arbor, Michigan 48109, United States*
Taryn Sleger − *Agios Pharmaceuticals, Inc., Cambridge, Massachusetts 02139, United States*
Bo Wang − *Agios Pharmaceuticals, Inc., Cambridge, Massachusetts 02139, United States*
Stefan Gross − *Agios Pharmaceuticals, Inc., Cambridge, Massachusetts 02139, United States*
Brandon N. Nicolay − *Agios Pharmaceuticals, Inc., Cambridge, Massachusetts 02139, United States*
Sebastien Ronseaux − *Agios Pharmaceuticals, Inc., Cambridge, Massachusetts 02139, United States*
Kaitlin Harvey − *Rogel Cancer Center and Department of Internal Medicine, University of Michigan, Ann Arbor, Michigan 48109, United States*
Yu Wang − *Rogel Cancer Center and Department of Internal Medicine, University of Michigan, Ann Arbor, Michigan 48109, United States*
Donna McEachern − *Rogel Cancer Center and Department of Internal Medicine, University of Michigan, Ann Arbor, Michigan 48109, United States*
Paul D. Kirchhoff − *Rogel Cancer Center and Department of Internal Medicine, University of Michigan, Ann Arbor, Michigan 48109, United States*
Zhaomin Liu − *Rogel Cancer Center and Department of Internal Medicine, University of Michigan, Ann Arbor, Michigan 48109, United States*
Jeanne Stuckey − *Life Sciences Institute, University of Michigan, Ann Arbor, Michigan 48109, United States*
Adriana E. Tron − *Agios Pharmaceuticals, Inc., Cambridge, Massachusetts 02139, United States*
Tao Liu − *Agios Pharmaceuticals, Inc., Cambridge, Massachusetts 02139, United States*

Complete contact information is available at: https://pubs.acs.org/10.1021/acs.jmedchem.1c00789

Author Contributions

[±]M.Z., A.A., S.X., and L.H. contributed equally. T.S, B.W., S.G., B.N.N., S.R., and A.E.T. designed and/or executed in vitro and in vivo studies. A.E.T. and T.L. contributed to writing and review of the manuscript.

Funding

This work is supported in part by the National Institutes of Health/National Cancer Institute (R01 CA208267 to S.W.), the Prostate Cancer Foundation (to S.W.), the Rogel Cancer Center Core Grant from the National Cancer Institutes, NIH (P30 CA046592), and a research contract from Agios Pharmaceuticals (to S.W.). Use of the Advanced Photon Source, an Office of Science User Facility operated for the U.S. Department of Energy (DOE) Office of Science by the Argonne National Laboratory, was supported by the U.S. DOE under Contract No. DE-AC02-06CH11357. Use of the LS-CAT Sector 21 was supported by the Michigan Economic Development Corporation and the Michigan Technology Tri-Corridor (Grant 085P1000817).

Notes

The authors declare the following competing financial interest(s): The University of Michigan has filed a number of patent applications on this class of menin inhibitors, which have been licensed to Medsyn Biopharma, LLC. S. Wang, M. Zhang, A. Aguilar, S. Xu, L. Huang, T. Xu, K. Zheng, D. McEachern, and J. Stuckey are co-inventors on one or more of these patents and receive royalties on these patents from the University of Michigan. S. Wang is a co-founder of Medsyn Biopharma LLC. The University of Michigan and S. Wang own stock in Medsyn. T.S, B.W, S.G., B.N.N., S.R., A.E.T and T.L are current or former employees and shareholders of Agios Pharmaceuticals, Inc.

■ ACKNOWLEDGMENTS

We thank G.W. A. Milne for critical reading and editing of the manuscript.

■ ABBREVIATIONS

ALL, acute lymphoblastic leukemia; AML, acute myeloid leukemia; DCM, dichloromethane; DIBAL-H, diisobutylaluminum hydride; DIPEA, *N*,*N*-diisopropylethylamine; ESI-MS, electrospray ionization mass spectrometry; EtOAc, ethyl acetate; FP, fluorescence polarization; MEN1, multiple endocrine neoplasia 1; MLL, mixed lineage leukemia protein; GSH, glutathione; PBS, phosphate buffered saline; PD, pharmacodynamics; rt, room temperature; SCID, severe combined immunodeficient; TFA, trifluoroacetic acid; UPLC, ultraperformance liquid chromatography

■ REFERENCES

(1) Dimartino, J. F.; Cleary, M. L. Mll rearrangements in haematological malignancies: lessons from clinical and biological studies. *Br. J. Haematol.* **1999**, *106*, 614−626.
(2) Marschalek, R. Mechanisms of leukemogenesis by MLL fusion proteins. *Br. J. Haematol.* **2011**, *152*, 141−154.
(3) Slany, R. K. The molecular biology of mixed lineage leukemia. *Haematologica* **2009**, *94*, 984−993.
(4) Meyer, C.; Burmeister, T.; Gröger, D.; Tsaur, G.; Fechina, L.; Renneville, A.; Sutton, R.; Venn, N. C.; Emerenciano, M.; Pombo-de-Oliveira, M. S.; Barbieri Blunck, C.; Almeida Lopes, B.; Zuna, J.; Trka, J.; Ballerini, P.; Lapillonne, H.; De Braekeleer, M.; Cazzaniga, G.; Corral Abascal, L.; van der Velden, V. H. J.; Delabesse, E.; Park, T. S.; Oh, S. H.; Silva, M. L. M.; Lund-Aho, T.; Juvonen, V.; Moore, A. S.; Heidenreich, O.; Vormoor, J.; Zerkalenkova, E.; Olshanskaya, Y.; Bueno, C.; Menendez, P.; Teigler-Schlegel, A.; zur Stadt, U.; Lentes, J.; Göhring, G.; Kustanovich, A.; Aleinikova, O.; Schäfer, B. W.; Kubetzko, S.; Madsen, H. O.; Gruhn, B.; Duarte, X.; Gameiro, P.; Lippert, E.; Bidet, A.; Cayuela, J. M.; Clappier, E.; Alonso, C. N.; Zwaan, C. M.; van den Heuvel-Eibrink, M. M.; Izraeli, S.; Trakhtenbrot, L.; Archer, P.; Hancock, J.; Möricke, A.; Alten, J.; Schrappe, M.; Stanulla, M.; Strehl, S.; Attarbaschi, A.; Dworzak, M.; Haas, O. A.; Panzer-Grümayer, R.; Sedék, L.; Szczepański, T.; Caye, A.; Suarez, L.; Cavé, H.; Marschalek, R. The MLL recombinome of acute leukemias in 2017. *Leukemia* **2018**, *32*, 273−284.
(5) Faber, J.; Krivtsov, A. V.; Stubbs, M. C.; Wright, R.; Davis, T. N.; van den Heuvel-Eibrink, M.; Zwaan, C. M.; Kung, A. L.; Armstrong, S. A. HOXA9 is required for survival in human MLL-rearranged acute leukemias. *Blood* **2009**, *113*, 2375−2385.
(6) Kumar, A. R.; Sarver, A. L.; Wu, B.; Kersey, J. H. Meis1 maintains stemness signature in MLL-AF9 leukemia. *Blood* **2010**, *115*, 3642−3643.
(7) Caslini, C.; Yang, Z.; El-Osta, M.; Milne, T. A.; Slany, R. K.; Hess, J. L. Interaction of MLL amino terminal sequences with menin is required for transformation. *Cancer Res.* **2007**, *67*, 7275−7283.
(8) Yokoyama, A.; Somervaille, T. C. P.; Smith, K. S.; Rozenblatt-Rosen, O.; Meyerson, M.; Cleary, M. L. The menin tumor suppressor protein is an essential oncogenic cofactor for MLL-associated leukemogenesis. *Cell* **2005**, *123*, 207−218.

(9) Chen, Y.-X.; Yan, J.; Keeshan, K.; Tubbs, A. T.; Wang, H.; Silva, A.; Brown, E. J.; Hess, J. L.; Pear, W. S.; Hua, X. The tumor suppressor menin regulates hematopoiesis and myeloid transformation by influencing Hox gene expression. *Proc. Natl. Acad. Sci. U. S. A.* **2006**, *103*, 1018−1023.
(10) Yokoyama, A.; Wang, Z.; Wysocka, J.; Sanyal, M.; Aufiero, D. J.; Kitabayashi, I.; Herr, W.; Cleary, M. L. Leukemia proto-oncoprotein MLL forms a SET1-like histone methyltransferase complex with menin to regulate Hox gene expression. *Mol. Cell. Biol.* **2004**, *24*, 5639−5649.
(11) Shi, A.; Murai, M. J.; He, S.; Lund, G.; Hartley, T.; Purohit, T.; Reddy, G.; Chruszcz, M.; Grembecka, J.; Cierpicki, T. Structural insights into inhibition of the bivalent menin-MLL interaction by small molecules in leukemia. *Blood* **2012**, *120*, 4461−4469.
(12) Murai, M. J.; Chruszcz, M.; Reddy, G.; Grembecka, J.; Cierpicki, T. Crystal structure of menin reveals binding site for mixed lineage leukemia (MLL) protein. *J. Biol. Chem* **2011**, *286*, 31742−31748.
(13) Cierpicki, T.; Grembecka, J. Challenges and opportunities in targeting the menin−MLL interaction. *Future Med. Chem.* **2014**, *6*, 447−462.
(14) Grembecka, J.; He, S.; Shi, A.; Purohit, T.; Muntean, A. G.; Sorenson, R. J.; Showalter, H. D.; Murai, M. J.; Belcher, A. M.; Hartley, T.; Hess, J. L.; Cierpicki, T. Menin-MLL inhibitors reverse oncogenic activity of MLL fusion proteins in leukemia. *Nat. Chem. Biol.* **2012**, *8*, 277−284.
(15) Borkin, D.; Pollock, J.; Kempinska, K.; Purohit, T.; Li, X.; Wen, B.; Zhao, T.; Miao, H.; Shukla, S.; He, M.; Sun, D.; Cierpicki, T.; Grembecka, J. Property focused structure-based optimization of small molecule inhibitors of the protein−protein interaction between menin and mixed lineage leukemia (MLL). *J. Med. Chem.* **2016**, *59*, 892−913.
(16) He, S.; Malik, B.; Borkin, D.; Miao, H.; Shukla, S.; Kempinska, K.; Purohit, T.; Wang, J.; Chen, L.; Parkin, B.; Malek, S. N.; Danet-Desnoyers, G.; Muntean, A. G.; Cierpicki, T.; Grembecka, J. Menin-MLL inhibitors block oncogenic transformation by MLL-fusion proteins in a fusion partner-independent manner. *Leukemia* **2016**, *30*, 508−513.
(17) Xu, Y.; Yue, L.; Wang, Y.; Xing, J.; Chen, Z.; Shi, Z.; Liu, R.; Liu, Y.-C.; Luo, X.; Jiang, H.; Chen, K.; Luo, C.; Zheng, M. Discovery of Novel Inhibitors Targeting the menin-mixed lineage leukemia interface using pharmacophore- and docking-based virtual screening. *J. Chem. Inf. Model.* **2016**, *56*, 1847−1855.
(18) He, S.; Senter, T. J.; Pollock, J.; Han, C.; Upadhyay, S. K.; Purohit, T.; Gogliotti, R. D.; Lindsley, C. W.; Cierpicki, T.; Stauffer, S. R.; Grembecka, J. High-affinity small-molecule inhibitors of the menin-mixed lineage leukemia (MLL) interaction closely mimic a natural protein−protein interaction. *J. Med. Chem.* **2014**, *57*, 1543−1556.
(19) Borkin, D.; Klossowski, S.; Pollock, J.; Miao, H.; Linhares, B. M.; Kempinska, K.; Jin, Z.; Purohit, T.; Wen, B.; He, M.; Sun, D.; Cierpicki, T.; Grembecka, J. Complexity of blocking bivalent protein−protein interactions: development of a highly potent inhibitor of the menin−mixed-lineage leukemia interaction. *J. Med. Chem.* **2018**, *61*, 4832−4850.
(20) Borkin, D.; He, S.; Miao, H.; Kempinska, K.; Pollock, J.; Chase, J.; Purohit, T.; Malik, B.; Zhao, T.; Wang, J.; Wen, B.; Zong, H.; Jones, M.; Danet-Desnoyers, G.; Guzman, M. L.; Talpaz, M.; Bixby, D. L.; Sun, D.; Hess, J. L.; Muntean, A. G.; Maillard, I.; Cierpicki, T.; Grembecka, J. Pharmacologic inhibition of the menin-MLL interaction blocks progression of mll leukemia in vivo. *Cancer Cell* **2015**, *27*, 589−602.
(21) Brzezinka, K.; Nevedomskaya, E.; Lesche, R.; Haegebarth, A.; ter Laak, A.; Fernández-Montalván, A. E.; Eberspaecher, U.; Werbeck, N. D.; Moenning, U.; Siegel, S.; Haendler, B.; Eheim, A. L.; Stresemann, C. Characterization of the menin-MLL interaction as therapeutic cancer target. *Cancers* **2020**, *12*, 201.
(22) Krivtsov, A. V.; Evans, K.; Gadrey, J. Y.; Eschle, B. K.; Hatton, C.; Uckelmann, H. J.; Ross, K. N.; Perner, F.; Olsen, S. N.; Pritchard, T.; McDermott, L.; Jones, C. D.; Jing, D.; Braytee, A.; Chacon, D.; Earley, E.; McKeever, B. M.; Claremon, D.; Gifford, A. J.; Lee, H. J.; Teicher, B. A.; Pimanda, J. E.; Beck, D.; Perry, J. A.; Smith, M. A.; McGeehan, G. M.; Lock, R. B.; Armstrong, S. A. A menin-mll inhibitor induces specific chromatin changes and eradicates disease in models of mll-rearranged leukemia. *Cancer Cell* **2019**, *36*, 660−673.e11.
(23) Klossowski, S.; Miao, H.; Kempinska, K.; Wu, T.; Purohit, T.; Kim, E.; Linhares, B. M.; Chen, D.; Jih, G.; Perkey, E.; Huang, H.; He, M.; Wen, B.; Wang, Y.; Yu, K.; Lee, S. C.-W.; Danet-Desnoyers, G.; Trotman, W.; Kandarpa, M.; Cotton, A.; Abdel-Wahab, O.; Lei, H.; Dou, Y.; Guzman, M.; Peterson, L.; Gruber, T.; Choi, S.; Sun, D.; Ren, P.; Li, L.-S.; Liu, Y.; Burrows, F.; Maillard, I.; Cierpicki, T.; Grembecka, J. Menin inhibitor MI-3454 induces remission in MLL1-rearranged and NPM1-mutated models of leukemia. *J. Clin. Invest.* **2020**, *130*, 981−997.
(24) Aguilar, A.; Zheng, K.; Xu, T.; Xu, S.; Huang, L.; Fernandez-Salas, E.; Liu, L.; Bernard, D.; Harvey, K. P.; Foster, C.; McEachern, D.; Stuckey, J.; Chinnaswamy, K.; Delproposto, J.; Kampf, J. W.; Wang, S. Structure-based discovery of m-89 as a highly potent inhibitor of the menin-mixed lineage leukemia (menin-MLL) protein−protein interaction. *J. Med. Chem.* **2019**, *62*, 6015−6034.
(25) Li, L.; Zhou, R.; Geng, H.; Yue, L.; Ye, F.; Xie, Y.; Liu, J.; Kong, X.; Jiang, H. Discovery of two aminoglycoside antibiotics as inhibitors targeting the menin−mixed lineage leukaemia interface. *Bioorg. Med. Chem. Lett.* **2014**, *24*, 2090−2093.
(26) Xu, S.; Aguilar, A.; Xu, T.; Zheng, K.; Huang, L.; Stuckey, J.; Chinnaswamy, K.; Bernard, D.; Fernández-Salas, E.; Liu, L.; Wang, M.; McEachern, D.; Przybranowski, S.; Foster, C.; Wang, S. Design of the first-in-class, highly potent irreversible inhibitor targeting the menin-MLL protein−protein interaction. *Angew. Chem., Int. Ed.* **2018**, *57*, 1601−1605.
(27) Zhou, H.; Liu, L.; Huang, J.; Bernard, D.; Karatas, H.; Navarro, A.; Lei, M.; Wang, S. Structure-based design of high-affinity macrocyclic peptidomimetics to block the menin-mixed lineage leukemia 1 (MLL1) protein−protein interaction. *J. Med. Chem.* **2013**, *56*, 1113−1123.
(28) Xu, S.; Aguilar, A.; Huang, L.; Xu, T.; Zheng, K.; McEachern, D.; Przybranowski, S.; Foster, C.; Zawacki, K.; Liu, Z.; Chinnaswamy, K.; Stuckey, J.; Wang, S. Discovery of M-808 as a highly potent, covalent, small-molecule inhibitor of the menin-MLL interaction with strong in vivo antitumor activity. *J. Med. Chem.* **2020**, *63*, 4997−5010.
(29) Larsen, S. D.; Grieco, P. A.; Fobare, W. F. Reactions of allylsilanes with simple iminium salts in water: A facile route to piperidines via a aminomethano desilylation-cyclization process. *J. Am. Chem. Soc.* **1986**, *108*, 3512−3513.
(30) Benoit, E.; Bueno, B.; Choinière, C.; Gagnon, A. First use of an organobismuth reagent in C(sp3)−S bond formation: Access to aryl cyclopropyl sulfides via copper-catalyzed S−Cyclopropylation of thiophenols using tricyclopropylbismuth. *J. Organomet. Chem.* **2019**, *893*, 72−77.
(31) Wang, S.; Altman, J.; Pettit, K.; Botton, S.; Walter, R.; Fenaux, P.; Burrows, F.; Tomkinson, B.; Martell, B.; Fathi, A. *115 Preliminary data on a phase 1/2A first in human study of the menin-KMT2A (MLL) inhibitor KO-539 in patients with relapsed or refractory acute myeloid leukemia*. Presented at: 2020 American Society of Hematology Annual Meeting and Exposition. December 5−8, 2020; Virtual. Abstract 115. https://ash.confex.com/ash/2020/webprogram/Paper134942.html.
(32) McGeehan, J. A first-in-class Menin-MLL1 antagonist for the treatment of MLL-r and NPM1 mutant leukemias. In *AACR Virtual Annual Meeting*; Presented at: the 2020 I; April 27−28, 2020. Abstract DDT01−01. https://www.abstractsonline.com/pp8/#!/9045/presentation/6808.
(33) Otwinowski, Z.; Minor, W., [20] Processing of X-ray diffraction data collected in oscillation mode. *In Methods in enzymology*;, Carter, C. W., Ed. Academic Press: San Diego, USA, 1997; *Vol. 276*, pp. 307−326.
(34) Vagin, A.; Teplyakov, A. MOLREP: an automated program for molecular replacement. *J. Appl. Crystallogr.* **1997**, *30*, 1022−1025.

https://doi.org/10.1021/acs.jmedchem.1c00789
J. Med. Chem. 2021, 64, 10333−10349

(35) Emsley, P.; Cowtan, K. Coot: model-building tools for molecular graphics. *Acta Cryst. D* **2004**, *60*, 2126−2132.
(36) Roversi, P.; Sharff, A.; Smart, O. S.; Vonrhein, C.; Womack, T. O. *BUSTER version 2.11.2 Cambridge*, United Kingdom: Global Phasing Ltd., 2011.
(37) Smart, O. S.; Womack, T. O.; Sharff, A.; Flensburg, C.; Keller, P.; Paciorek, W.; Vonrhein, C.; Bricogne, G. *GRADE, 1.2.13*; Global Phasing Ltd.: Cambridge, United Kingdom, 2017.
(38) *Molecular Operating Environment (MOE)*, 2019.01; Chemical Computing Group ULC: 1010 Sherbrooke St. West, Suite #910, Montreal, QC, Canada, H3A 2R7, 2019.

https://doi.org/10.1021/acs.jmedchem.1c00789
J. Med. Chem. 2021, 64, 10333−10349